

# **ON THE MECHANISM OF HETEROGENEOUS LIQUID-PHASE OXIDATION OF CUMENE, CYCLOHEXENE AND TETRALIN**

A Thesis Submitted  
In Partial Fulfilment of the Requirements  
for the Degree of  
**MASTER OF TECHNOLOGY**

By  
**L. V. GOPALA KRISHNA**

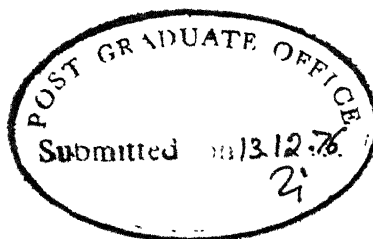
to the  
**DEPARTMENT OF CHEMICAL ENGINEERING  
INDIAN INSTITUTE OF TECHNOLOGY, KANPUR**  
December, 1976

CHE-1976--M--KRI--MEC

L.I.T. LIBRARY  
CENTRAL LIBRARY

Acc. No. **A 50811**

12 AUG 1977



[ii]

CERTIFICATE

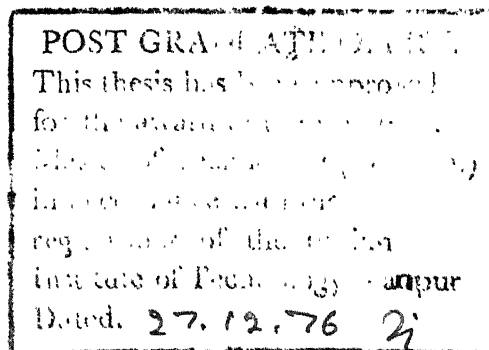
Certified that this work has been carried out under our supervision and it has not been submitted elsewhere for a degree.

*M. S. Rao*  
M.S. Rao  
Assistant Professor  
Department of Chemical Engg.  
Indian Institute of Technology  
Kanpur-208016, India

Date

*R. D. Srivastava*  
R.D. Srivastava  
Assistant Professor  
Department of Chemical Engg.  
Indian Institute of Technol  
Kanpur-208016, India

Date



### ACKNOWLEDGEMENTS

Extreme gratitude and thanks are due to Dr. R.D. Srivastava for his able guidance in experimentation and interpretation of the results. The author is highly grateful to Dr. M.S. Rao for introducing him to the field of statistical analysis.

The author expresses thanks to Professor D.Devaprabhakara for the help rendered in chemical analysis. Messrs K.Rajagopala and G.S. Hegde of Chemistry Department are acknowledged for the care taken in analysing the chemical samples.

The author is indebted to Mr. K.K.Rao who helped a long way in computer programming and Messrs Subhash C.Shenoy and Anil K. Agarwal for their help in getting over the practical difficulties.

Thanks are due to Herdillia Chemicals for providing cumene required for the work.

Lastly, the author is thankful to his colleagues and chemical engineering staff for their encouragement and cooperation.

Author

CONTENTS

	Page
List of Figures	v
List of Appendices	vi
Abstract	vii
1. INTRODUCTION	1
1.1 Literature Survey	1
1.2 Present Work	9
2. EXPERIMENTAL	10
2.1 Materials	10
2.2 Apparatus	10
2.3 Procedure	13
2.4 Analytical	15
3. RESULTS AND DISCUSSION	16
3.1 Initiation	16
3.2 Effect of Catalyst Weight	16
3.3 Effect of Hydrocarbon Concentration	21
3.4 Decomposition of Hydroperoxide	27
3.5 Reaction Mechanism	27
3.6 Derivation of Kinetic Expression	33
4. STATISTICAL ANALYSIS	36
4.1 Estimation of Parameters and Their Confidence Intervals	36
4.2 Residual Analysis	37
5. CONCLUSIONS	42
References	43
Appendices	45

---

---

LIST OF FIGURES

FIGURE		Page
1.	Schematic Diagram of the Experimental Set-up	11
2.	Oxygen Absorption versus Time for Cumene	17
3.	Rate vs Catalyst Ratio for Cumene	19
4.	Rate vs Catalyst Ratio for Cyclohexene	20
5.	Rate vs Catalyst Ratio for Tetralin	22
6.	Oxygen Absorption vs Time for Different Cumene Concentrations	24
7.	Rate vs Cumene Concentration	25
8.	Rate vs Cyclohexene Concentration	26
9.	Rate vs Tetralin Concentration	28
10.	Cumene Hydroperoxide decomposition vs Catalyst Ratio	29
11.	Cyclohexene Hydroperoxide Decomposition vs Catalyst Ratio	30
12.	Tetralin Hydroperoxide Decomposition vs Catalyst Ratio	31
13.	Residual vs Cumene Concentration	39
14.	Residual vs Cyclohexene Concentration	40
15.	Residual vs Tetralin Concentration	41

---

LIST OF FIGURES

FIGURE		Page
1.	Schematic Diagram of the Experimental Set-up	11
2.	Oxygen Absorption versus Time for Cumene	17
3.	Rate vs Catalyst Ratio for Cumene	19
4.	Rate vs Catalyst Ratio for Cyclohexene	20
5.	Rate vs Catalyst Ratio for Tetralin	22
6.	Oxygen Absorption vs Time for Different Cumene Concentrations	24
7.	Rate vs Cumene Concentration	25
8.	Rate vs Cyclohexene Concentration	26
9.	Rate vs Tetralin Concentration	28
10.	Cumene Hydroperoxide decomposition vs Catalyst Ratio	29
11.	Cyclohexene Hydroperoxide Decomposition vs Catalyst Ratio	30
12.	Tetralin Hydroperoxide Decomposition vs Catalyst Ratio	31
13.	Residual vs Cumene Concentration	39
14.	Residual vs Cyclohexene Concentration	40
15.	Residual vs Tetralin Concentration	41

---

LIST OF APPENDICES

## APPENDIX A

## Cumene Runs

- Table A-1 Oxygen Consumption vs Time for Different Catalyst Ratios for Cumene
- A-2 Oxygen Consumption vs Time for Different Cumene Concentrations
- A-3 Cumene Hydroperoxide Decomposition Runs

## APPENDIX B

## Cyclohexene Runs

- Table B-1 Oxygen Consumption vs Time
- B-2 Oxygen Consumption vs Time for Different Concentrations
- B-3 Cyclohexene Hydroperoxide Decomposition Runs

## APPENDIX C

## Tetralin Runs

- Table C-1 Oxygen Consumption vs Time for Different Catalyst Ratios
- C-2 Oxygen Consumption vs Time for Different Tetralin Concentrations
- C-3 Tetralin Hydroperoxide Decomposition Runs

## APPENDIX D

## Statistical Analysis

- D-1 Computer Program Listings for Estimation of Parameters and  $[X^T X]^{-1}$
- D-2 Confidence Interval Calculation for Parameter Estimates
- D-3
- Table D-1 Residual Analysis for Cumene
- D-2 Residual Analysis for Cyclohexene
- D-3 Residual Analysis for Tetralin
-



## 1. INTRODUCTION

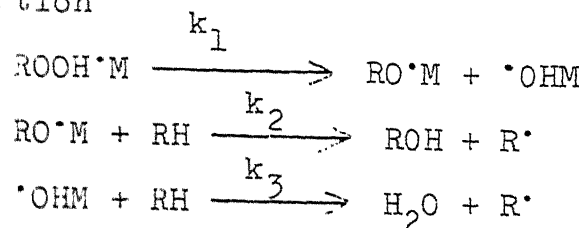
Recently, the heterogeneous catalytic oxidation of arenes namely, cumene and tetralin and the cyclic compound, cyclohexene, have been subjects of numerous investigations [1-10]. The mechanisms of these reactions have drawn considerable academic and industrial attention. In the past five years there has been considerable advancement in the elucidation of the mechanisms of oxidations of cumene and cyclohexene. A brief literature survey on the mechanisms of oxidation of these compounds is presented in the following section:

### 1.1 Literature Survey:

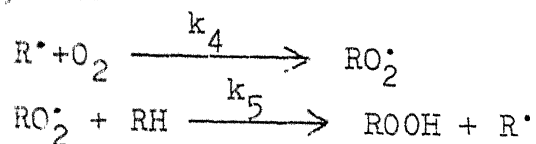
Mukherjee and Graydon [1] have studied the liquid-phase oxidation of tetralin (1,2,3,4-tetrahydronaphthalene) using both soluble and insoluble catalysts and compared the reaction rates. Oxides of nickel, manganese, and copper were found to be extremely active while those of aluminium and zinc were inactive. Rates of oxidation were measured in the temperature range of 45-90°C. The initial product of oxidation reaction was found to be tetralin hydroperoxide which decomposed further into tetralone and tetralol. A ketone:alcohol ratio of 2:1 was observed in the product with most of the catalysts. It was further noticed that a critical hydroperoxide to catalyst ratio existed below which the reaction did not proceed.

Kinetic studies have been made with four of the best catalysts, and the reaction mechanism proposed is as follows:

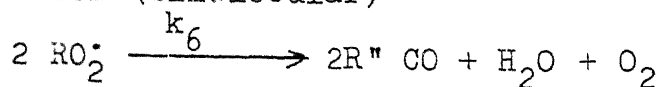
Initiation



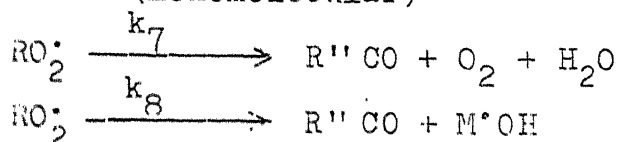
Propagation



Termination (bimolecular)



Termination (monomolecular)



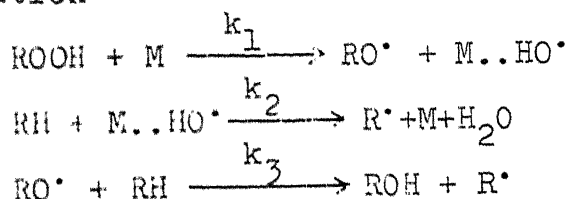
with  $\text{R} = \text{C}_6\text{H}_5\text{C}(\text{CH}_3)_2$  and  $\text{M}$  = active site of the catalyst surface

Van Ham et al. [2] have found that the use of silver catalyst showed a significant lowering of the activation energy in the oxidation of cumene. They also found a pronounced increase in the oxidation rate by using silver instead of silver-gold alloy as the catalyst.

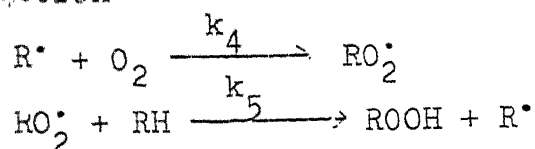
Neuburg et al. [3] studied the heterogeneous liquid-phase oxidation of cyclohexene using manganese dioxide as the catalyst. The decomposition of cyclohexenyl hydroperoxide was also studied. The dependence of initial rate on the catalyst

amount had been studied both for oxidation and decomposition reactions and a degenerate chain branching mechanism had been postulated by the authors. Hydroperoxide which was produced in the propagation step was decomposed on the solid generating the free radicals necessary for the initiation of the chains. Cyclohexenol and cyclohexenone were produced in the initiation and termination steps. Above a critical catalyst to hydrocarbon ratio, no oxidation reaction was observed. At that critical composition, the rate of hydroperoxide decomposition was equal to its rate of formation. The length of the chain decreased to a low value with increasing catalyst to hydrocarbon ratios. The mechanism adapted is as follows:

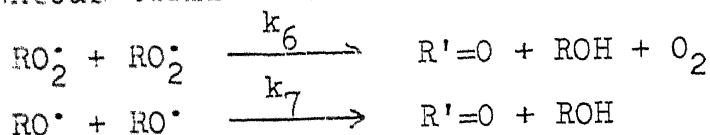
#### Initiation



#### Propagation



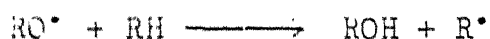
#### Homogeneous termination



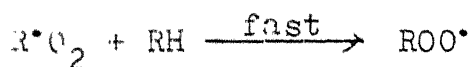
The oxidation of cumene and the decomposition of cumene hydroperoxide on silver, copper and platinum were studied by Casemier et al. [4]. Cumene hydroperoxide dissolved in dodecane

rapidly decomposed by platinum and appreciably by silica gel or by silver in the absence of gaseous oxygen, but virtually no decomposition was observed with unsupported silver in an oxygen atmosphere. The oxidation of cumene to cumene hydroperoxide showed a completely different picture; this oxidation was strongly catalyzed by silver, whereas copper, gold and platinum did not catalyze the reaction. For the cumene oxidation with silver a free radical (presumably  $\text{ROO}^\bullet$ ) was detected in the reaction mixture by EPR spectroscopy. The reaction mechanism assumed diatomic oxygen to be adsorbed on the silver surface. The proposed mechanism is as follows:

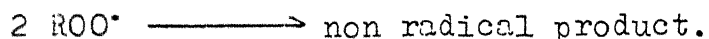
#### Initiation



#### Propagation



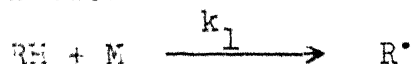
#### Termination



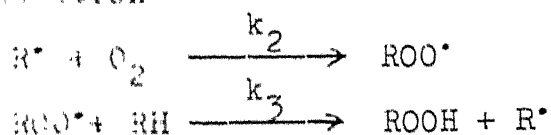
Verma and Graydon [5] studied the heterogeneous catalytic oxidation of cumene in liquid phase. The investigation was made at  $80^\circ\text{C}$  with molecular oxygen. Cobalt<sup>II,III</sup> oxide,  $\text{MnO}_2$ ,  $\text{NiO}$  and  $\text{Cu}_2\text{O}$  were used as catalysts. Detailed studies of the effect of catalyst weight, hydrocarbon concentration and initial

hydroperoxide concentration on the rate of oxidation were conducted employing cobalt<sup>II,III</sup> oxide as the catalyst. The oxygen absorption rate was found to be 0.4 power with respect to the catalyst weight, and 1.5 power with respect to the cumene concentration. The concentrations of the main products of oxidation of cumene, viz., cumene hydroperoxide, dimethyl phenyl carbinol and acetophenone were found to depend on the weight of the catalyst. Reaction mechanisms and rate expressions for the oxidation of cumene were proposed. The mechanisms are illustrated below:

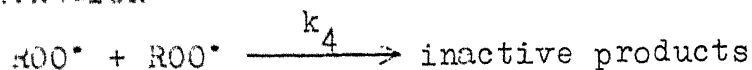
Initiation



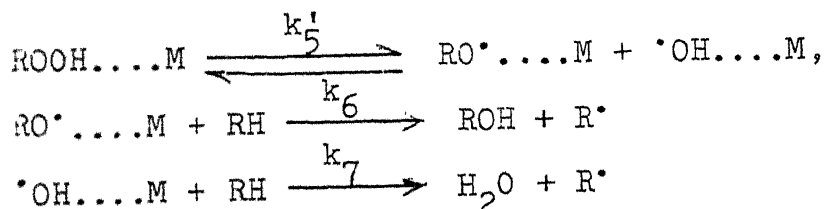
Propagation



Termination



The above mechanism was postulated when there was no hydrogen peroxide present in cumene. The effect of the initial hydrogen peroxide would be felt in the initiation reaction and a possible mechanism proposed was:



Neuburg et al. [6,7] conducted a detailed investigation on the oxidation of cyclohexene and decomposition of cyclohexene hydroperoxide. The liquid-phase decomposition as also the oxidation of cyclohexene hydroperoxide in cyclohexene [6] had been studied in the temperature range of 40 - 70°C using three types of  $\text{MnO}_2$  with different specific surfaces as catalysts. The influence of initial hydroperoxide concentration catalyst weight to liquid volume ratio and temperature were studied in each case. It was postulated that the hydroperoxide formed an equilibrium complex with the catalyst which further decomposed to yield free radicals. The initial activity of oxides decreased during the reaction and the observed decay in the rate of hydroperoxide decomposition had been attributed mainly to the deactivation of catalyst surface. The decomposition products were cyclohexenol, cyclohexenone and water. The number of moles of alcohol formed was higher than the number of moles of ketone in each case. In the oxidation study, reaction periods upto 60 min. were used to study the initial activity of the catalyst. The maximum rate of cyclohexene oxidation was 0.5 order with respect to the catalyst in the region of low catalyst weight to hydrocarbon ratios. A much lower order was found for higher ratios. Above a critical amount of catalyst, the oxidation was completely inhibited due to the quantitative decomposition of hydroperoxide. The maximum oxidation rate was proved to be first order with

Neuburg et al. [6,7] conducted a detailed investigation on the oxidation of cyclohexene and decomposition of cyclohexene hydroperoxide. The liquid-phase decomposition as also the oxidation of cyclohexene hydroperoxide in cyclohexene [6] had been studied in the temperature range of 40 - 70°C using three types of  $\text{MnO}_2$  with different specific surfaces as catalysts. The influence of initial hydroperoxide concentration catalyst weight to liquid volume ratio and temperature were studied in each case. It was postulated that the hydroperoxide formed an equilibrium complex with the catalyst which further decomposed to yield free radicals. The initial activity of oxides decreased during the reaction and the observed decay in the rate of hydroperoxide decomposition had been attributed mainly to the deactivation of catalyst surface. The decomposition products were cyclohexenol, cyclohexenone and water. The number of moles of alcohol formed was higher than the number of moles of ketone in each case. In the oxidation study, reaction periods upto 60 min. were used to study the initial activity of the catalyst. The maximum rate of cyclohexene oxidation was 0.5 order with respect to the catalyst in the region of low catalyst weight to hydrocarbon ratios. A much lower order was found for higher ratios. Above a critical amount of catalyst, the oxidation was completely inhibited due to the quantitative decomposition of hydroperoxide. The maximum oxidation rate was proved to be first order with

respect to the concentration of cyclohexene. The oxidation rate was of zero order with respect to the initial hydroperoxide concentration in the range of  $3 \times 10^{-3}$  to 0.5gmole/liter, giving support to the theory that free radicals were produced from the slow decomposition of the catalyst-hydroperoxide complex. Oxidation products such as cyclohexenol and cyclohexenone inhibited the oxidation rate when they were initially present in concentrations greater than 50  $\mu$ mole/ml. Apparent activation energies for the oxidation ranged between 11.4 and 13.0 Kcal/mole. Product distribution studies showed that cyclohexenol and cyclohexenone were produced in nearly equal amounts. A degenerating chain branching mechanism was proposed in which the catalyst played an important role in the initiation and termination steps. Rate equations derived from this mechanism explained quantitatively the experimental observations.

Panayotova et al. [9] worked on the role of metallic copper in the oxidation of cumene to cumene hydroperoxide. They reported that at moderate temperatures copper protects cumene hydroperoxide against decomposition. Copper corrosion takes place upon continuous processing of raw material, particularly at high temperatures. Interaction between the metal extracted into reaction medium and cumene hydroperoxide lead to intense decomposition of cumene hydroperoxide.

Srivastava and Srivastava [8] investigation the liquid phase oxidation of cumene with  $\text{Cr}_2\text{O}_3$ ,  $\text{MnO}_2$  and  $\text{Fe}_2\text{O}_3$  catalysts



in the temperature range of 70 - 90°C. Similar to the earlier finding of Varma and Graydon, the present authors observed a critical hydroperoxide to catalyst ratio, below which the reaction did not proceed. Effects of catalyst weight and hydrocarbon concentration on the rate of oxidation were studied in detail. The apparent activation energy for the overall oxidation was calculated to be 9.8 Kcal/g mole. A reaction mechanism had been proposed and the rate expression derived was in good agreement with the experimental data.

Agarwal and Srivastava [10] studied the kinetics and catalytic behaviour of NiO supported on alumina and activated carbon and also  $\text{Ni MoO}_4$  supported on alumina in the liquid phase oxidation of cumene. The catalysts had been characterized by means of DTA, TGA, X-ray, IR and BET studies. Detailed studies of the concentrations of main products along with effect of catalyst weight, and hydrocarbon concentration on the rate of oxidation were conducted at 80°C employing these supported catalysts. A reaction mechanism was proposed in which the catalyst plays an important role in the initiation and termination steps. Rate equations derived were in good agreement with the experimental data. It was observed that use of carbon as a support instead of alumina (NiO catalysts) induced increased activity, lower activation energies, and shifted the limiting oxidation rate to lower catalyst amount.

It has been established that, for the heterogeneous liquid phase oxidation of cumene, cyclohexene and tetralin catalyzed by transition metal oxides, there is a critical weight of catalyst above which the rate of oxidation drops catastrophically [1,3,5,8], which suggested that the rates of formation and destruction of hydroperoxide became equal [7]. A general mechanism explaining the simultaneous formation and destruction of hydroperoxide in the oxidation of cyclohexene has recently been proposed by Neuburg et al. [7], and used by Agarwal and Srivastava [10] to explain the kinetics of cumene oxidation. However, very few data have been presented for these systems in the region where inhibition was effective.

## 1.2 Present Work:

In the present work  $\text{MnO}_2$  catalyzed oxidations of cumene, cyclohexene and tetralin in the region where inhibition was effective, have been studied at the temperatures of 80, 60, and 65°C respectively. The results favor the view that these catalyzed oxidations involve simultaneous formation and destruction of hydroperoxide. Also the chain branched character of the generation of free radicals is confirmed.

---

## 2. EXPERIMENTAL

### 2.1 Materials:

Cumene, cyclohexene and tetralin were obtained from Herdillia Chemicals, Koch-Light (England) and Riedel De Haen Ag (Germany), respectively. Cumene and cyclohexene were further distilled fractionally.

Monochlorobenzene of Sarabhai M.Chemicals was used as inert solvent for varying the concentration of hydrocarbons.

Hydroperoxides of cumene, cyclohexene and tetralin were prepared separately by the thermal oxidation of the respective hydrocarbons at 60°C using  $\text{MnO}_2$  as the catalyst.

Oxygen and nitrogen were supplied by Indian Oxygen Limited, Kanpur. Nitrogen was used as an inert for the decomposition runs.

$\text{MnO}_2$  catalyst was supplied by BDH (India) Limited, Bombay.

### 2.2 Apparatus:

The apparatus was essentially similar to that used by Bolland [11] for the thermal oxidation of ethyl linoleate.

The apparatus consisted of a graduated gas-burette. The burette was 50 cm long and 1 cm inner diameter with both ends open. The bottom was connected to a mercury reservoir through a polythene tubing as shown in Figure 1.

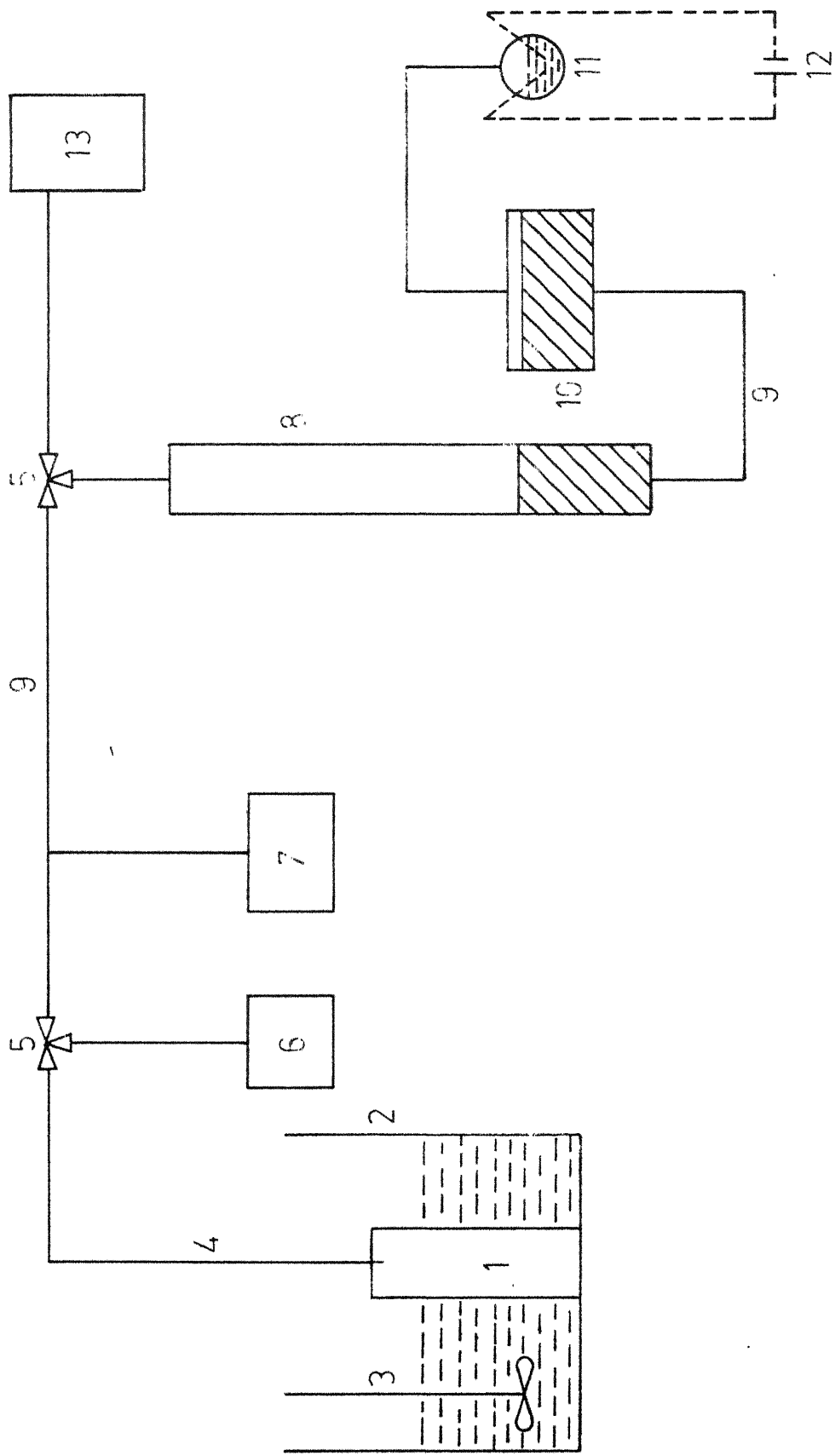


Fig. 1 - Schematic diagram of experimental set-up.

KEY TO FIGURE 1

- 1 : B 55/54 Glass Joint Reactor
- 2 : Constant Temperature Water Bath
- 3 : Remi Stirrer
- 4 : Rubber Tubing
- 5 : Three-way Stop Cock
- 6 : Connection to Vacuum Pump through Trap
- 7 : Mercury Manometer
- 8 : Gas-Burette With Mercury
- 9 : Polythene Tubing
- 10 : Mercury Reservoir
- 11 : Oxalic Acid Container
- 12 : 12V Battery
- 13 : Connection to Gas Cylinder

Oxygen line and the reactor were connected to the gas-burette by polythene tubing through a three-way stop-cock. The reactor consisted of a B 55/54 glass joint. The male joint was connected to a three-way stop-cock, which in turn was connected to a vacuum line and mercury manometer. The reactor volume was 400 cc. A vacuum pump was used for evacuating the system. The reactor was placed in a constant temperature water bath. Water in the bath was stirred by a ~~semi~~-stirrer. The bath was heated by a 2 KW heater. An on-off relay and a contact thermometer of range 0-300°C were used to maintain the desired bath temperature.

Efficient stirring of the reaction mixture was achieved by using a magnetic stirrer. The stirrer consisted of a glass-covered iron piece.

### 2.3 Procedure:

All the oxidation runs were performed using  $\text{MnO}_2$  as the catalyst at the corresponding temperatures mentioned below for different systems.

Cumene	80°C
Cyclohexene	60°C
Tetralin	65°C

The experimental procedure consisted of the following steps:

1. The water-bath was switched on and allowed to reach the desired steady-state temperature, which normally took half an hour.

2. The desired catalyst amount was taken in the clean and dry reactor. Then the iron stirring piece was dropped in the reactor.

3. 25 ml of the hydrocarbon were added in the reactor.

4. The reactor was connected to the gas-burette and the system was evacuated by means of a vacuum pump.

5. The system was filled with oxygen.

6. The reactor was placed in the bath.

7. After fifteen minutes the magnetic stirrer was switched on and change in the burette reading was recorded.

8. After the run the products were allowed to cool down to room temperature and then centrifuged for fifteen minutes at 800 RPM in order to separate the catalyst from the products.

#### Hydroperoxide Decomposition Runs:

For the decomposition runs, the hydroperoxide solution of the respective hydrocarbon of known concentration was added, together with the desired amount of  $\text{MnO}_2$  catalyst to the reactor, under nitrogen. All the decomposition runs were performed for thirty minutes.

The samples were analyzed as described below:

## 2.4 Analytical

The main products of decomposition were the respective hydroperoxide, alcohol and ketone. In the case of cumene, cumene hydroperoxide, cumyl alcohol and acetophenone were the products. Similarly for the decomposition of cyclohexene, cyclohexene hydroperoxide, cyclohexenol and cyclohexenone were the products, while tetralin hydroperoxide, tetralol and tetralone were the products in the decomposition of tetralin. The following methods were used for analyzing the various products of the decomposition runs.

### Hydroperoxide:

The hydroperoxide content in each case was estimated by iodometric method [12]. 40 ml of isopropyl alcohol and 5 ml sample were mixed and refluxed. The mixture was cooled to room temperature and 10 ml isopropyl alcohol saturated with sodium iodide were added and refluxed. The liberated iodide was titrated against sodium thiosulphate solution.

### Alcohol:

Cumyl alcohol and peroxide were converted to phenol by treating the sample with sulfuric acid and hydrogen peroxide[13]. Bromide-bromate method was used to estimate phenol [17]. 5 ml of the sample was treated with 50 ml of 0.1N of potassium bromate-bromide solution and 5 ml of HCl. The mixture was shaken and allowed to stand for 15 min. Two grams of potassium iodide were added. The liberated iodine was titrated with 0.1N sodium thiosulphate using 2 ml of starch indicator.

### Ketone:

The ketone concentration in the product was determined using Perkin-Elmer-137 IR spectrophotometer by studying the absorption at  $1700\text{ cm}^{-1}$ .



### 3. RESULTS AND DISCUSSION

The symbols RH, ROOH and ROH are used in general for hydrocarbons, hydroperoxides and alcohols, respectively. All the relevant experimental data for the oxidation and decomposition runs are presented in Appendices A, B, and C respectively.

In order to study the effect of hydrocarbon concentration in the region where inhibition was effective, it was necessary to study the oxidation rate as a function of the catalyst ratio for all the three systems. The catalyst ratio is defined as the weight of the catalyst in grams divided by the volume of the hydrocarbon in ml.

#### 3.1 Initiation:

The reaction did not commence when the cumene oxidation was performed at 80°C in absence of the catalyst or any free radical initiator. When some hydroperoxide was added to the system the oxygen consumption started immediately. Therefore, to initiate the reaction both catalyst and hydroperoxide were necessary in all cases. Hydroperoxide concentration to catalyst ratio of approximately  $2.5 \times 10^{-4}$  gmole/lit g was used in all the three cases.

#### 3.2 Effect of Catalyst Weight:

##### Oxidation of Cumene:

The amount of oxygen absorbed versus time of oxidation for cumene at 80°C is shown in Figure 2. Data were obtained

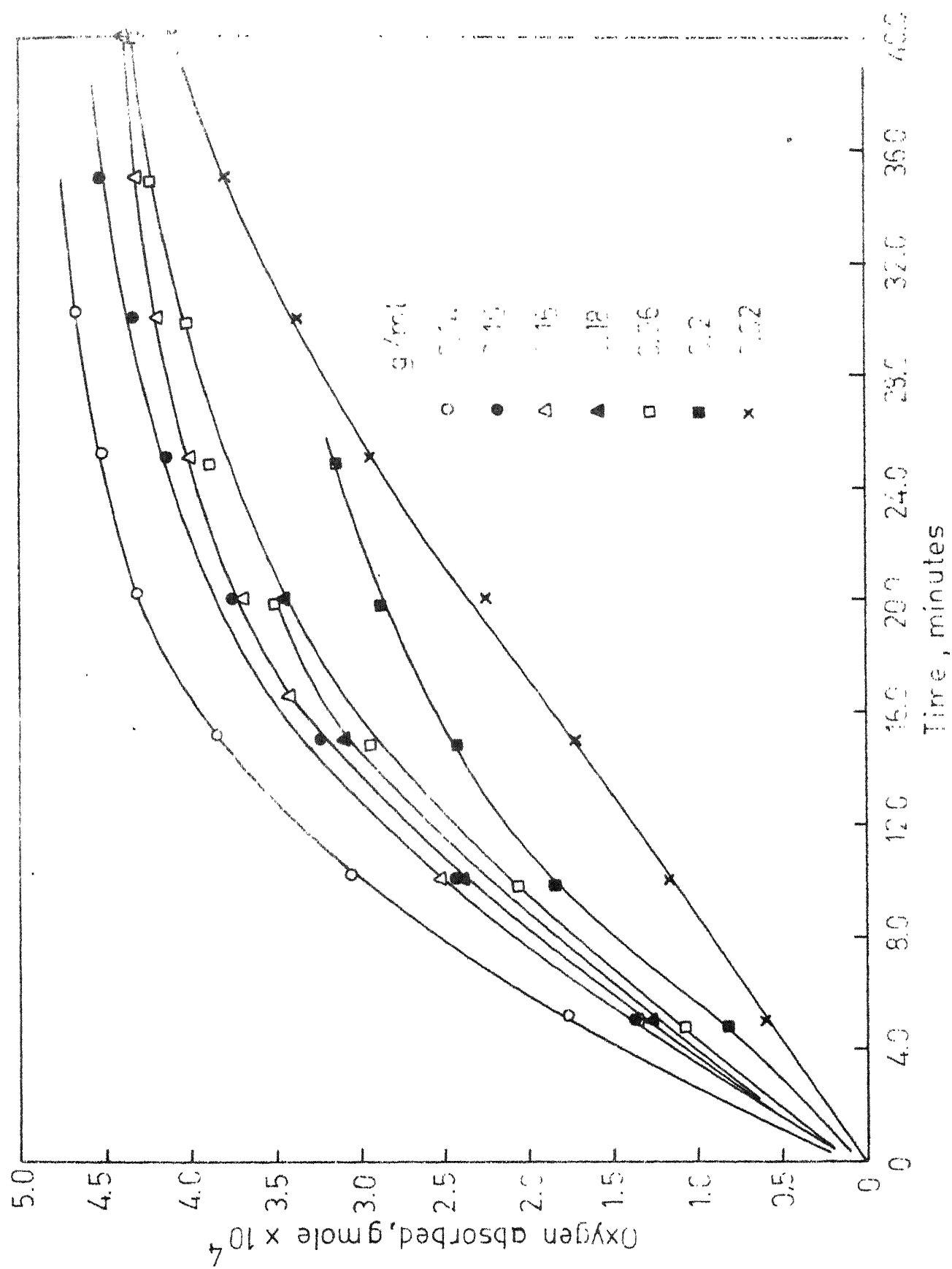


Fig. 2 -Oxygen absorption curves for cumene at 80°C for different  $\text{MnO}_2$  catalyst weights per 1 ml of cumene.

on the rate of oxygen absorption for various catalyst weight to hydrocarbon volume ratios ranging from 0.02 to 0.2 gram of catalyst per ml. of hydrocarbon. The initial rate obtained for 0.02 g/ml was  $1.7 \times 10^{-7}$  g.mole/sec. Srivastava and Srivastava [8] observed an oxygen absorption rate of  $1.3 \times 10^{-7}$  g mole/sec under the same conditions.

The rate of oxygen absorption versus catalyst weight is shown in Figure 3. It was observed that the rate of oxygen absorption was maximum at 0.14 g/ml. A further increase in the catalyst weight resulted in the decrease of rate of oxygen absorbed. This behaviour was observed by Srivastava and Srivastava [8] as well as by Varma and Graydon [5]. The value above which the rate declines is referred to as the critical catalyst amount. Srivastava and Srivastava [8] established that the critical catalyst amount was unaffected by variation in temperature over the temperature range 70 - 80°C.

#### Oxidation of Cyclohexene:

The data recorded in Table B.1 of Appendix B represent the consumption of oxygen with time for various catalyst ratios with  $\text{MnO}_2$  as a catalyst at 60°C. A detailed study was performed to obtain the rate of oxygen absorbed for various catalyst ratios ranging from 0.08 to 0.4 g/ml. Figure 4 shows the rate against catalyst ratio. As in the case of cumene the rate of oxidation dropped rapidly after 0.2 g/ml. Similar observation was made by Neuburg et al. [3]. They observed a

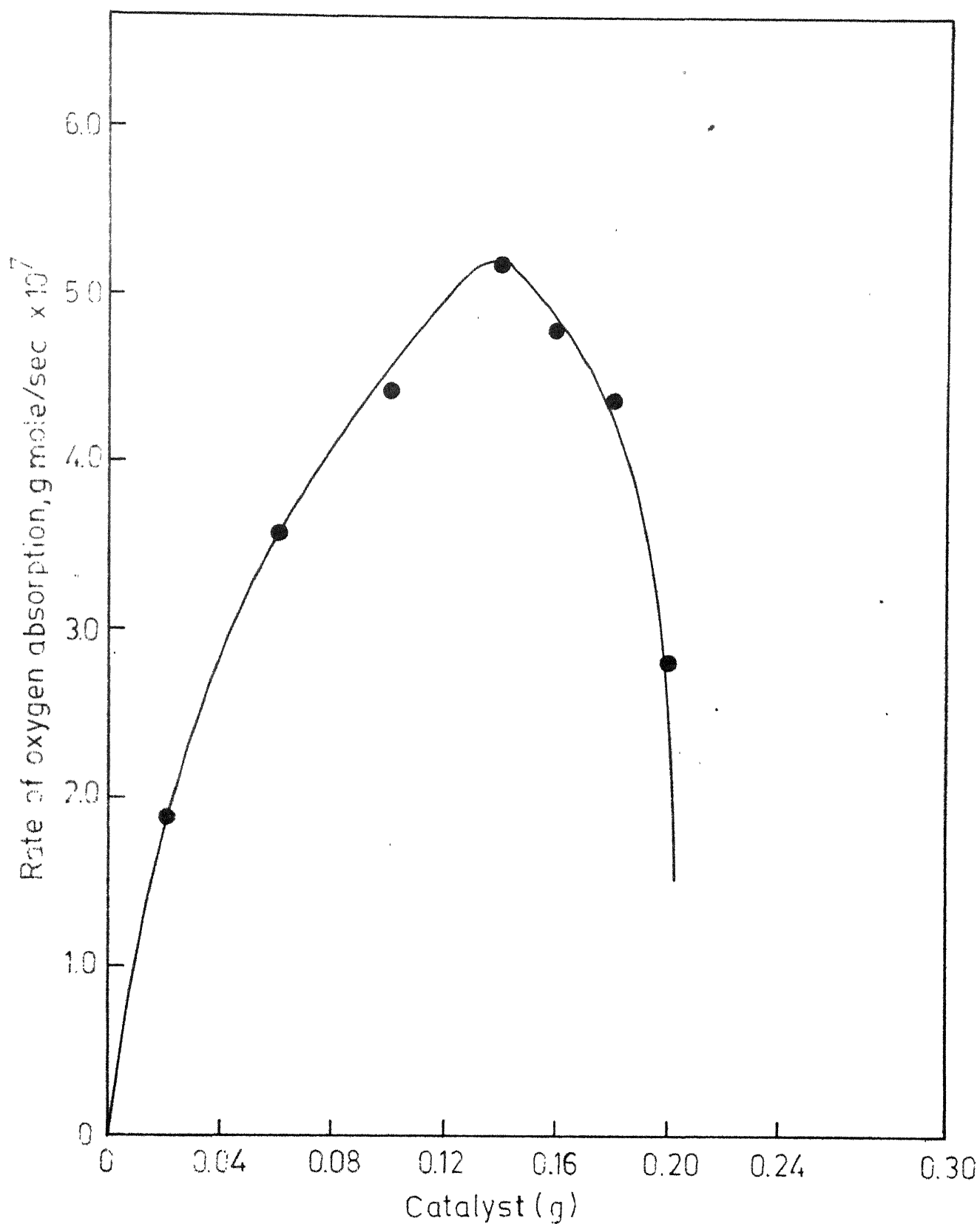


Fig. 3 - Measured rates of oxygen absorption for 1ml. of cumene at 80°C as a function of weight of MnO<sub>2</sub> catalyst.

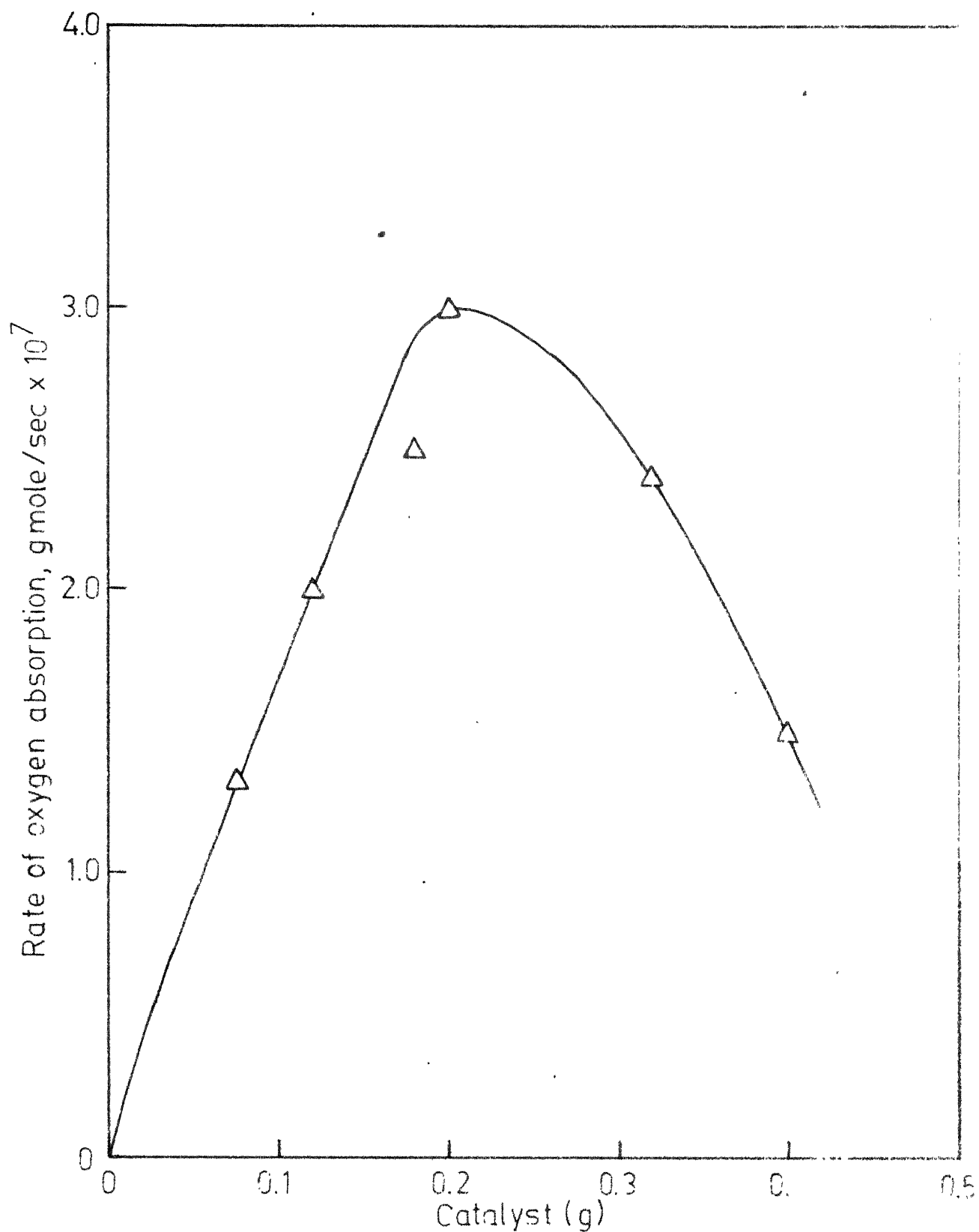


Fig. 4 - Measured rates of oxygen absorption for 1ml. cyclohexene at 60°C as a function of MnO<sub>2</sub> catalyst weight.

decline in rate at 0.16 g/ml under the same conditions. In the present study the maximum rate observed was  $3 \times 10^{-7}$  g.mole/sec. while Neuburg et al. [3] found  $7 \times 10^{-7}$  g.mole/sec.

#### Oxidation of Tetralin:

The oxidation of tetralin was carried out using the same  $\text{MnO}_2$  catalyst at  $65^\circ\text{C}$ . The amount of oxygen absorbed versus time is shown in Table C-1 (Appendix C). Oxygen absorption was studied at catalyst ratios of 0.2, 0.4, 0.8, 0.9 and 1.0 g/ml. The rate data were plotted against catalyst ratios as shown in Figure 5. As seen the behaviour is similar to those of oxidation of cumene and cyclohexene. Mukherjee and Graydon [1] also observed the same behaviour while investigating this reaction.

Thus, in all the three cases of oxidation of cumene, cyclohexene, and tetralin there is a catalyst ratio above which oxidation rates decline. It has already been established that before the break-point the rates of oxidation in the presence of transition metal oxides proceed with approximately 0.5 and 1 power with respect to catalyst ratio and hydrocarbon concentration, respectively.[2,5,8,10].

#### 3.3 Effect of Hydrocarbon Concentration in the Inhibiting Region:

The influence of cumene, cyclohexene and tetralin concentrations on the respective rate of oxidation was studied with the mixture of the corresponding hydrocarbon with

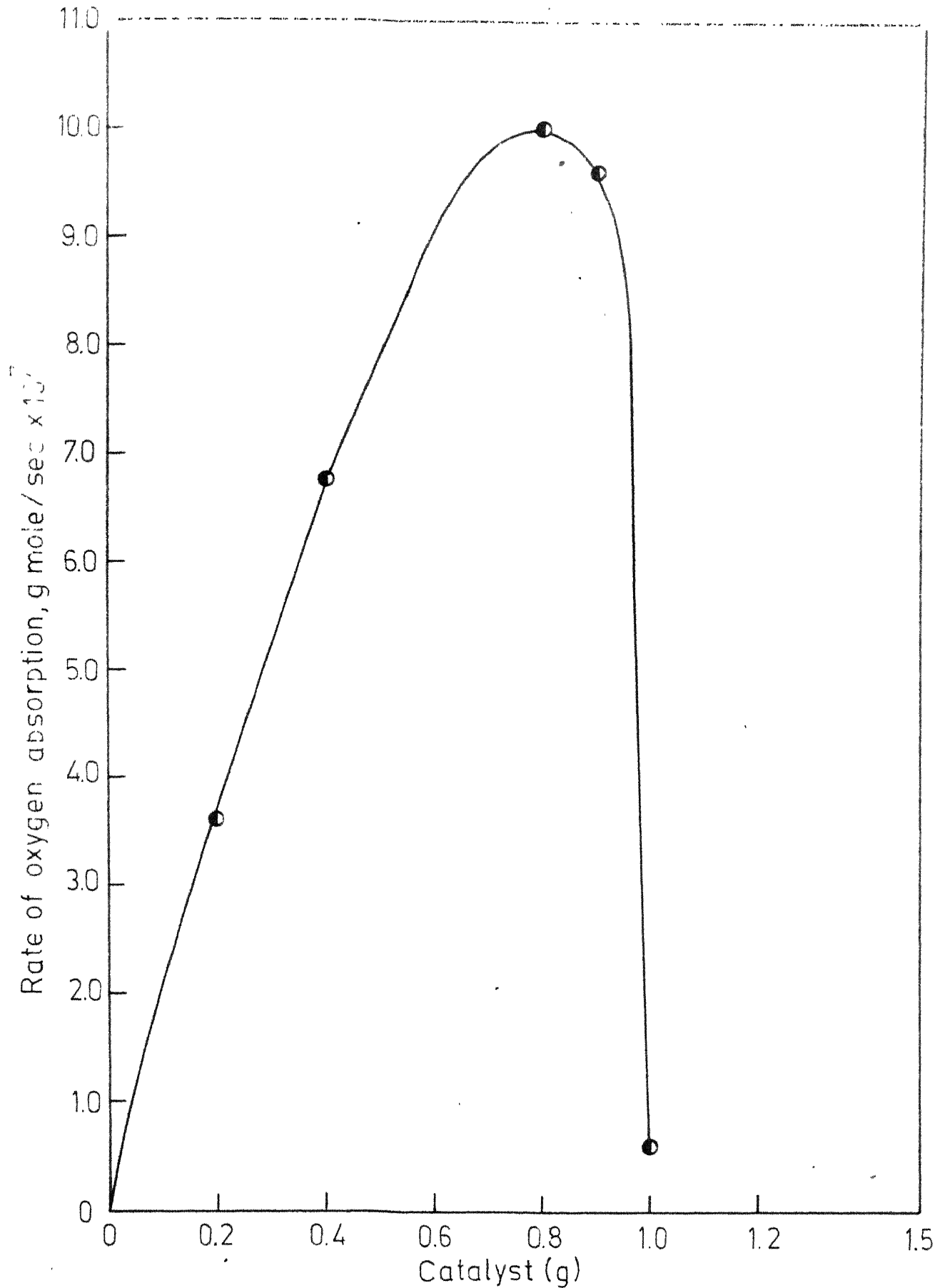


Fig. 5 -Measured rates of oxygen absorption for 1ml. of tetralin at 65°C as a function of  $\text{MnO}_2$  catalyst weight.

monochlorobenzene at catalyst ratios chosen from the inhibiting region.

#### Cumene:

Runs were conducted for three different catalyst ratios 0.16, 0.18 and 0.2 g/ml (Figure 3). Figure 6 represents a typical plot of oxygen absorbed versus time at various hydrocarbon concentrations for the catalyst ratio 0.16 g/ml. The data for 0.18 and 0.2 g/ml. are presented in Table A-2 (Appendix A). The rates were calculated and plotted against the cumene concentration, on a log-log graph as shown in Figure 7. It is interesting to note that the orders obtained were 2.3, 2.1, and 2.2 with respect to hydrocarbon concentration for the catalyst ratios 0.16, 0.18 and 0.2 g/ml, respectively. It shows that the rate dependence with respect to the cumene concentration in the inhibiting region is approximately 2.

#### Cyclohexene:

As in the case of cumene the cyclohexene concentration was varied and runs were conducted for four different concentrations. The catalyst ratio chosen was 0.22 g/ml (Figure 4). Table B.2 (Appendix B) represents the data of oxygen absorbed versus time. The rate of oxidation as a function of cyclohexene concentration is shown in Figure 8 on a log-log plot. The rate dependence with respect to cyclohexene concentration was found to be 1.7.



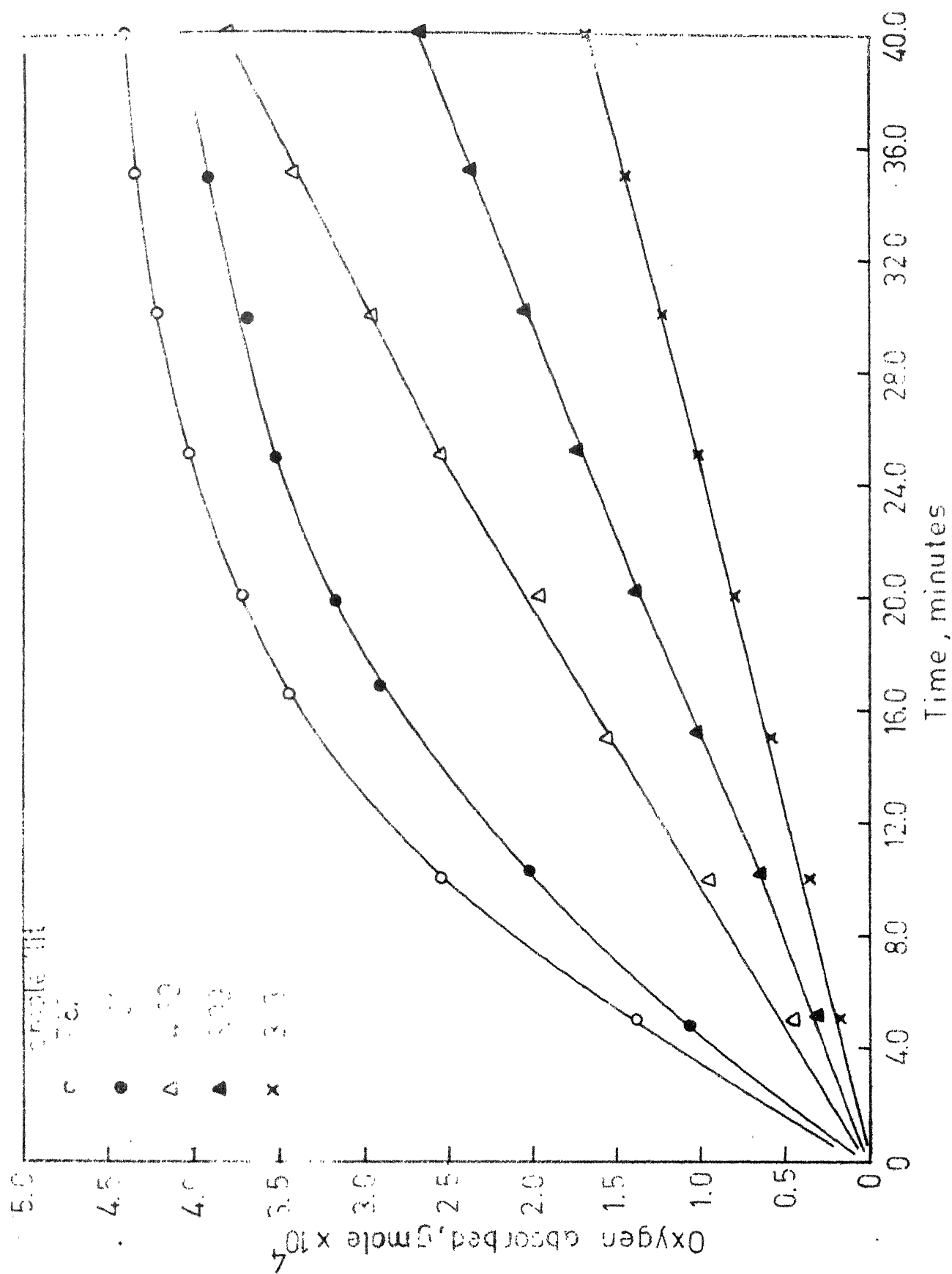


Fig. 5 - Oxygen absorption curves for catalyst ratio 0.15g MnO<sub>2</sub> per ml. of cumene at 80°C as a function of cumene concentration (g mole/lit.)

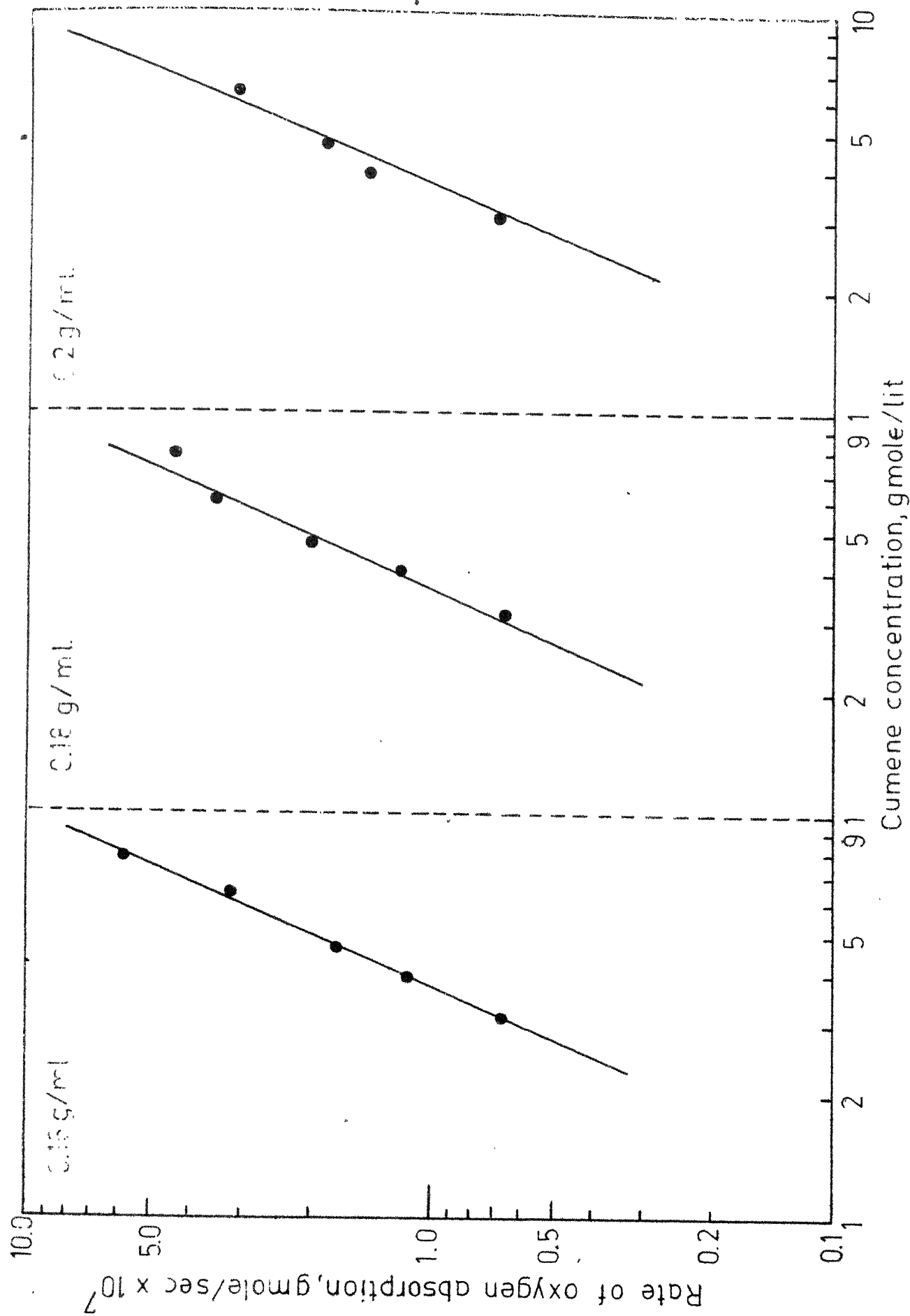


Fig. 7 - Rate dependence with respect to cumene concentration for catalyst weights 0.16g, 0.18g & 0.2g per 1ml of cumene at 80°C

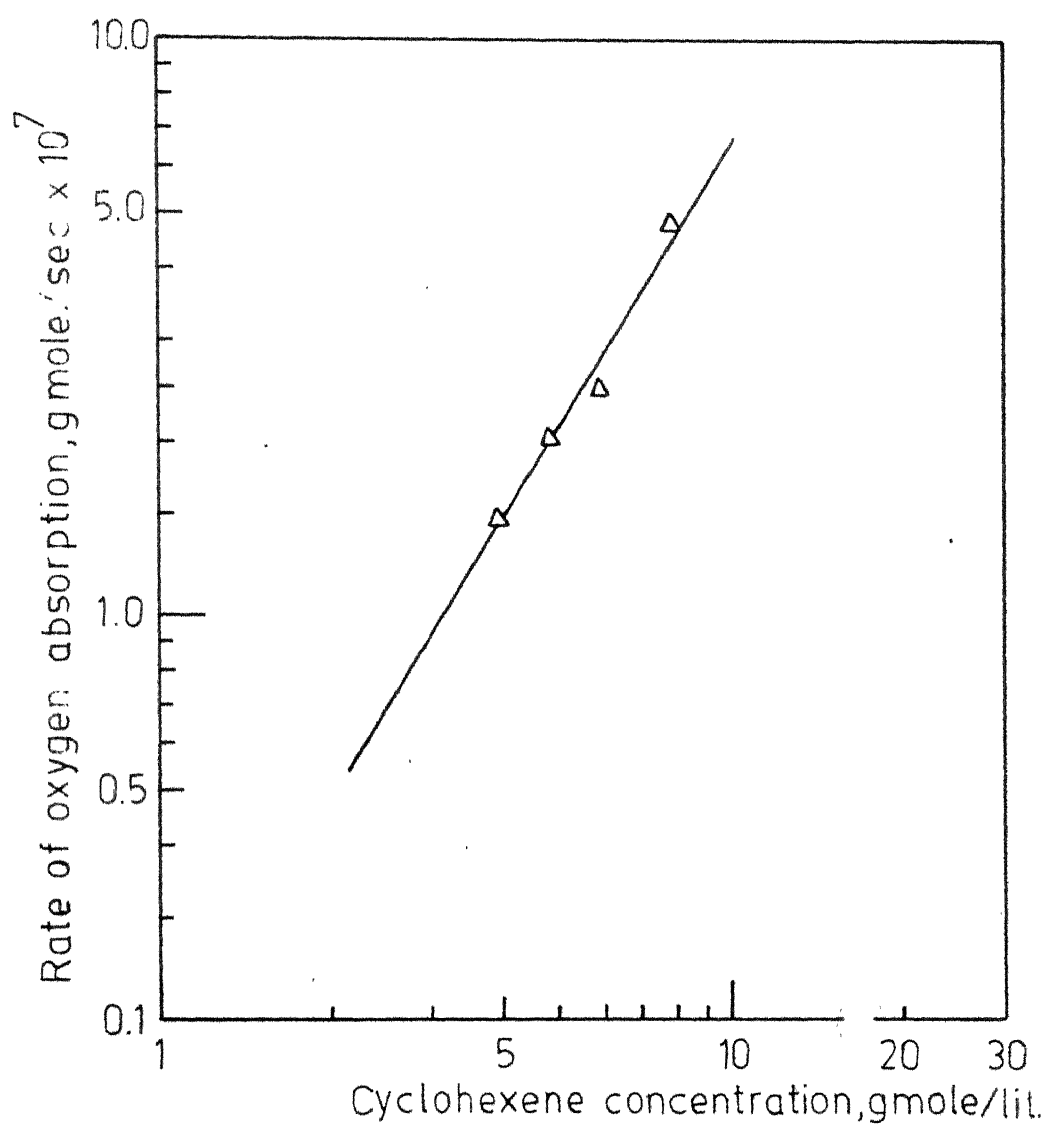


Fig. 8 - Rate dependence with respect to cyclohexene concentration for 0.22 g  $\text{MnO}_2$  per 1ml. of cyclohexene at  $60^\circ\text{C}$ .

### Tetralin:

In case of tetralin a catalyst ratio of 0.9 g/ml was employed. This was again chosen from the inhibiting region (Figure 5). The oxygen absorption data are shown in Table C.2 (Appendix C). In Figure 9 rates of oxygen absorption are plotted against hydrocarbon concentrations on a log-log plot. The order with respect to hydrocarbon concentration was found to be 2.1.

### 3.4 Decomposition of Hydroperoxide:

The decomposition reactions of the hydroperoxides of cumene, cyclohexene and tetralin were studied for various catalyst ratios at the temperatures of 80, 60 and 65°C, respectively. The decomposition products observed were alcohol, ketone and water. The data are presented in Tables A.3, B.3 and C.3. Figures 10-12 represent the percentage of hydroperoxide decomposed against various catalyst ratios using a single initial hydroperoxide concentration in each case. It is interesting to observe that the percentage decomposition increases with the increasing catalyst ratio upto the break-in-point and then shows a decrease on further increase in the catalyst ratio.

### 3.5 Reaction Mechanism:

The experimental observations made during the study of oxidation of cumene, cyclohexene and tetralin may be

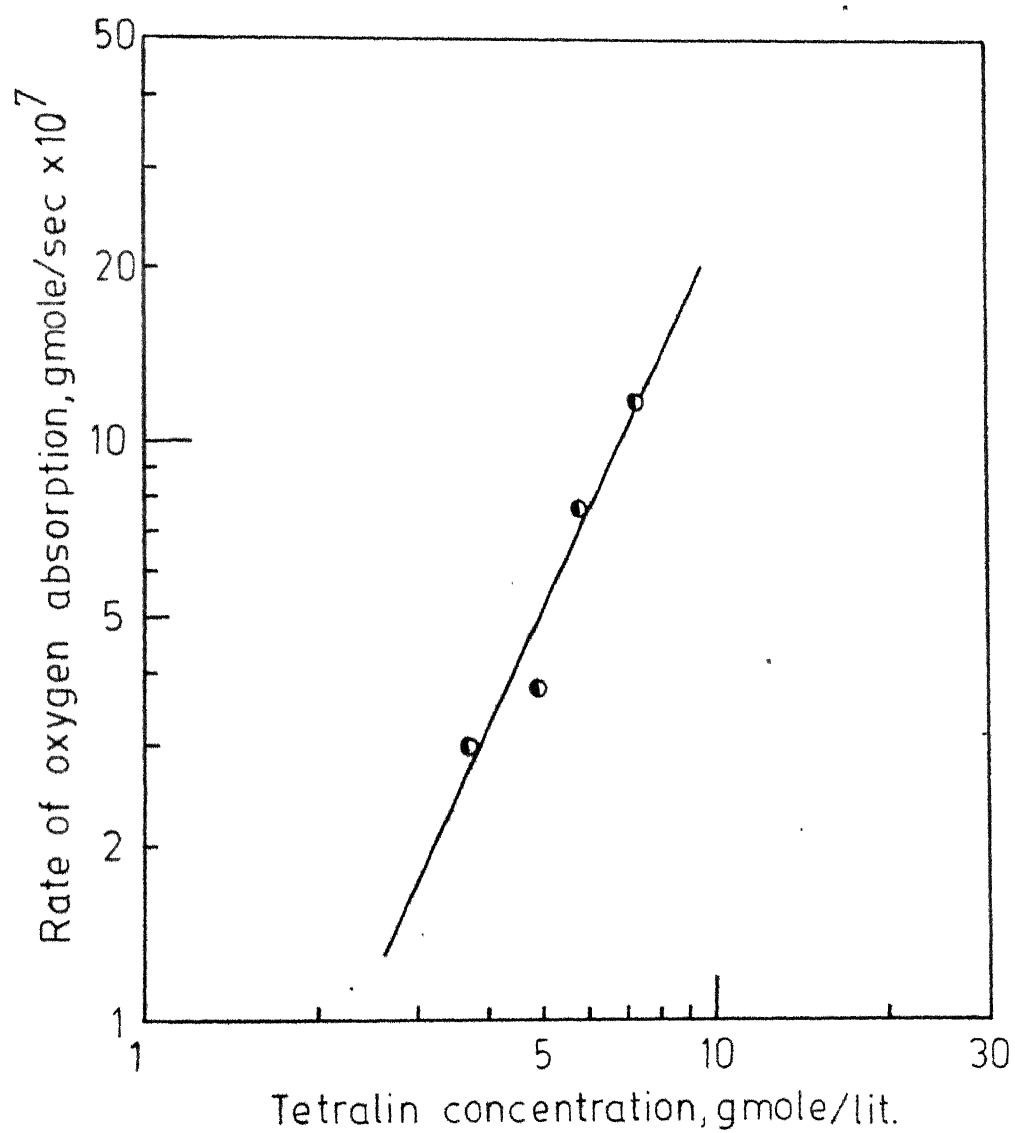


Fig. 9 -Rate dependence with respect to tetralin concentration for 0.9 g MnO<sub>2</sub> per 1 ml. of tetralin at 65°C.

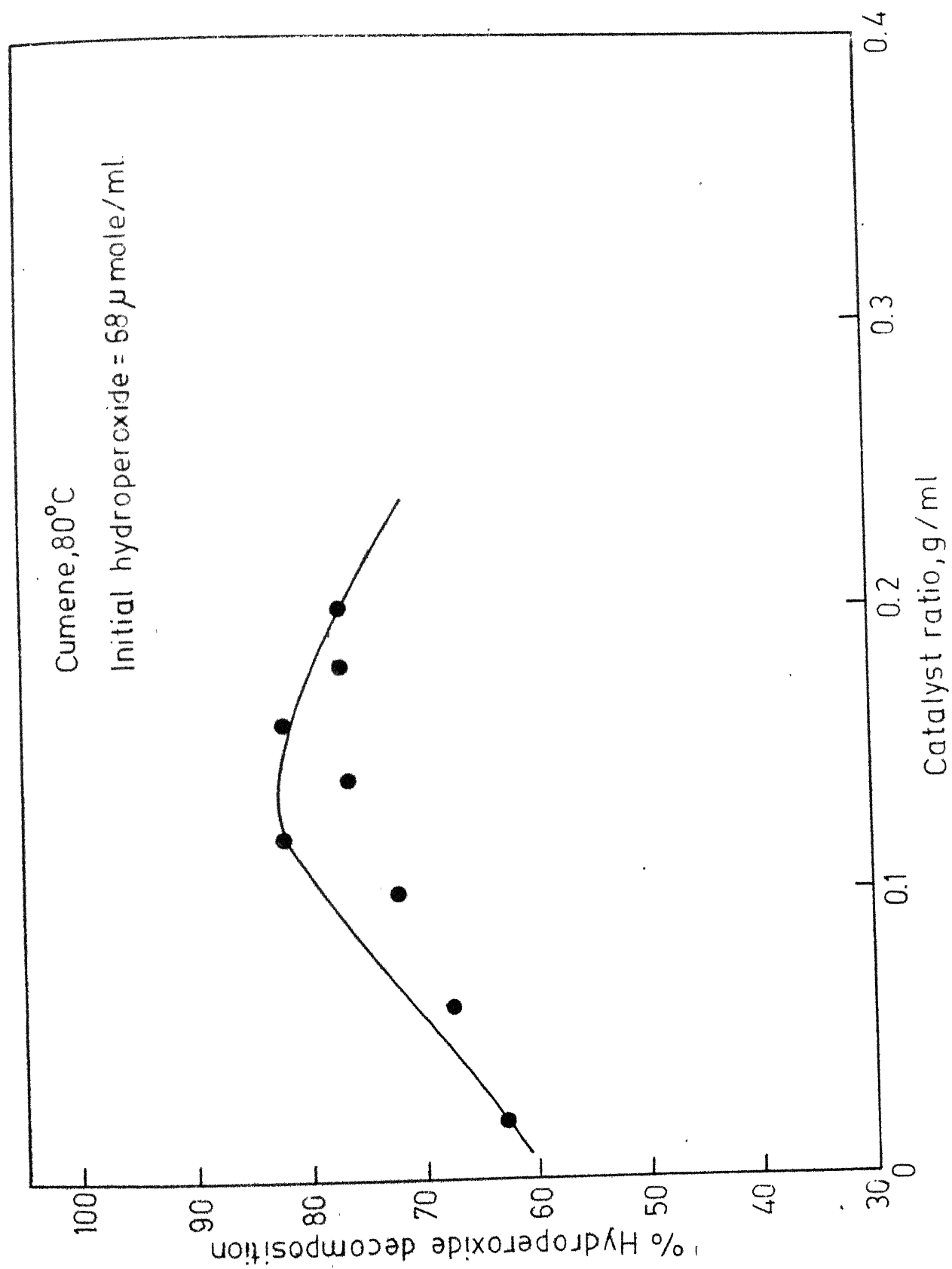


Fig. 10 -Percentage decomposition of cumene hydroperoxide against catalyst ratio ; time -30 min.

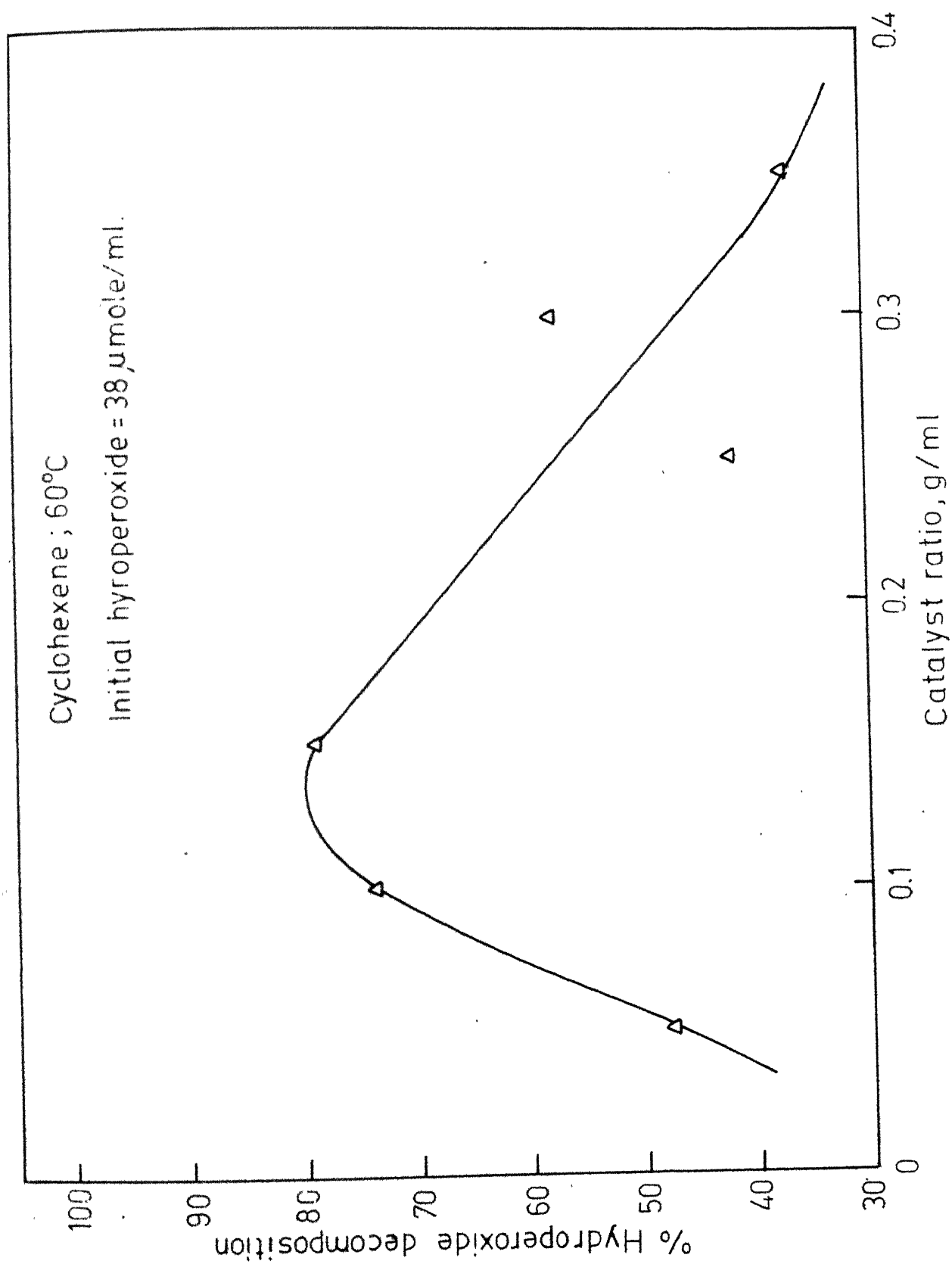


Fig. 11 - Percentage decomposition of cyclohexene hydroperoxide against catalyst ratio ; time - 30 min.

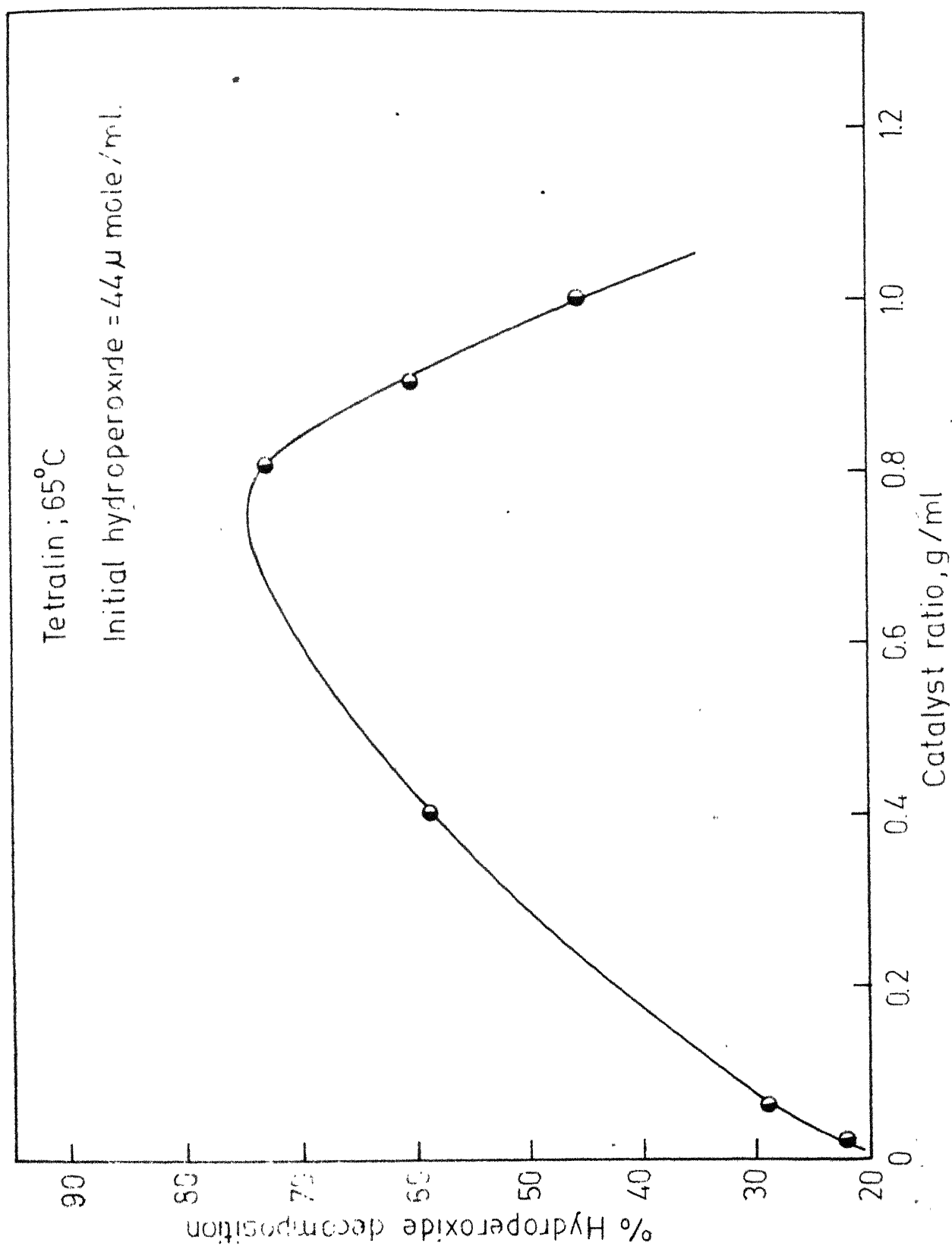


Fig. 12 - Percentage decomposition of tetralin hydroperoxide against catalyst ratio ; time - 30 min.

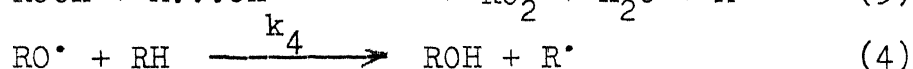
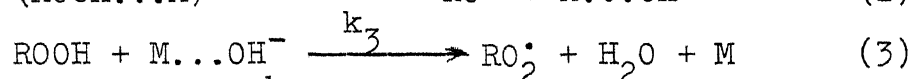
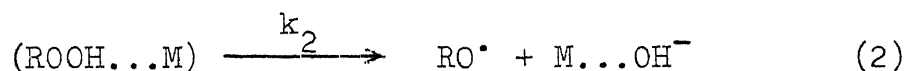
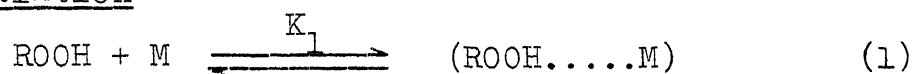


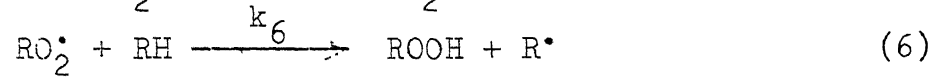
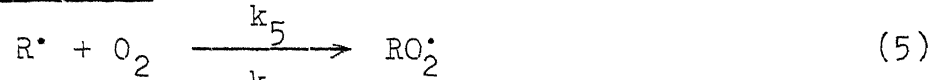
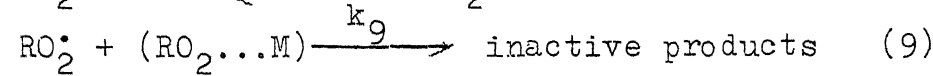
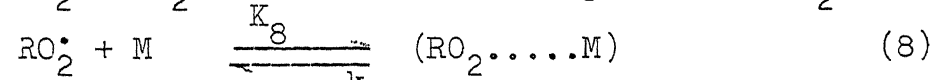
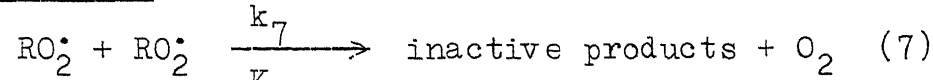
summarized in general as follows:

- (a) For lower catalyst ratios the rate of oxidation increases with increasing catalyst ratio. For higher catalyst ratios, there is a decline in the rate of oxidation which is referred to as the inhibiting region.
- (b) For the catalyst ratios in the inhibiting region, the rate of oxidation is approximately second order with respect to the hydrocarbon concentration.
- (c) The decomposition of hydroperoxide in all the three cases increases with increasing catalyst ratio, passes through a maximum and then declines suddenly.

Based on the observations made in the present study and from the established facts that, before the limiting region, the rate dependence is 0.5 order with respect to catalyst weight and first order with respect to hydrocarbon concentration, a general mechanism as proposed by Neuburg et al. [7] is described below:

Initiation



Propagation:Termination:3.6 Derivation of Kinetic Expression:

At steady-state, the rate of initiation of free radicals is equal to the rate of consumption of free radicals.

Therefore: Rate of initiation of free radicals

$$R_i = 2 k_7 [RO_2^\bullet]^2 + k_9 [RO_2^\bullet] [RO_2 \dots M] \quad (10)$$

Reaction (8) is under equilibrium.

$$\text{Therefore: } k_8 = \frac{[ROO \dots M]}{[RO_2^\bullet] [M]} \quad (11)$$

$$[ROO \dots M] = k_8 [RO_2^\bullet] [M]$$

$$R_i = 2 k_7 [RO_2^\bullet]^2 + k_8 k_9 [RO_2^\bullet]^2 [M]$$

$$= [RO_2^\bullet]^2 (2 k_7 + k_8 k_9 [M])$$

$$[RO_2^\bullet] = \left( \frac{R_i}{2k_7 + k_8 k_9 [M]} \right)^{\frac{1}{2}} \quad (12)$$

Rate of oxygen consumption is given by

$$-\frac{d[O_2]}{dt} = k_6 [RO_2^\bullet] [RH] + R_i - k_7 [RO_2^\bullet]^2 \quad (13)$$

$$= k_6 \left( \frac{R_i}{2k_7 + k_8 k_9 [M]} \right)^{\frac{1}{2}} [RH] + R_i \left( 1 - \frac{k_7}{2k_7 + k_8 k_9 [M]} \right) \quad (14)$$

Assuming formation of oxygen through termination is negligible

$$-\frac{d[O_2]}{dt} = k_6 \left( \frac{R_i}{2 k_7 + k_8 k_9 [M]} \right)^{\frac{1}{2}} [RH] \quad (15)$$

If the termination of peroxy radicals on the catalyst surface is negligible compared to biradical termination

$$-\frac{d[O_2]}{dt} = k_6 \left( \frac{R_i}{2 k_7} \right)^{\frac{1}{2}} [RH] \quad (16)$$

It may be assumed that  $R_i$  is proportional to the amount of catalyst. This rate expression (Eq. 16) clearly accounts for the observations of 0.5 and 1 order with respect to the catalyst ratio and the hydrocarbon concentration, respectively.

When the limiting rate condition is reached, the rate of formation of hydroperoxide by reaction (6) becomes equal to the rate of decomposition on the catalyst surface,  $R_d$ . Hence the net rate of formation of hydroperoxide is

$$\frac{d[ROOH]}{dt} = k_6 \left( \frac{R_i}{2 k_7 + k_8 k_9 [M]} \right)^{\frac{1}{2}} - R_d = 0 \quad (17)$$

$$\text{Let } R_i = \alpha R_d \quad (18)$$

where,  $\alpha$  is the fraction of hydroperoxide decomposed.

From equations(17) and (18), solving for  $R_i$  give

$$R_i = \frac{k_6^2 \alpha^2 [RH]^2}{2k_7 + k_8 k_9 [M]} \quad (19)$$

By substituting the value of  $R_i$  in Equation (14), the limiting rate of oxygen consumption becomes

$$-\left(\frac{d[O_2]}{dt}\right)_\infty = \frac{\alpha k_6^2 [RH]^2}{2k_7+k_8k_9[M]} \left[1+\alpha\left(1 - \frac{k_7}{2k_7+k_8k_9[M]}\right)\right] \quad (20)$$

For small value of  $\alpha$  the limiting rate of oxidation is given by

$$-\left(\frac{d[O_2]}{dt}\right)_\infty = \frac{\alpha k_6^2 [RH]^2}{2k_7+k_8k_9[M]} \quad (21)$$

Therefore, under limiting condition the oxidation rate must show a second order dependence on the hydrocarbon concentration. The experimental observations for all the three systems cumene, cyclohexene and tetralin give a rate dependence of approximately 2. The observations are, therefore, in good conformity with the rate expression derived. The similarity in the kinetic behaviour of the three systems may be due to formation of resonance stabilized radical species. Therefore, it is envisaged that a single mechanism satisfactorily explains the kinetic behaviour observed for all these systems.

---

#### 4. STATISTICAL ANALYSIS OF THE DATA

In order to further substantiate the model a statistical analysis was done. The statistical treatment involved estimation of parameters for the three systems under study, establishing confidence intervals [14] for the parameters and then a residual analysis [15].

##### 4.1 Estimation of Parameters and Their Confidence Intervals:

The parameter estimation was essentially based on the minimization of the sum of squares between the expected and the experimental responses with a suitable convergence criterion. Rosenbrock [16] optimization program was used for the minimization. IBM 1800 and IBM 7044 computers were used. The method is of direct-search type. An initial estimate was used to start with. The program was tested for convergence using Banana function,

$$F = 25 (x_2 - x_1)^2 + (1 - x_1)^2$$

For a fast convergence and simplification the non-linear model was reduced to a three parameter one as follows:

$$-\frac{d[O_2]}{dt} = \frac{b_1 [RH]^2}{b_2 + b_3 [M]}$$

where,  $b_1 = \alpha k_6$

$$b_2 = 2 k_7^2$$

$$b_3 = k_8 k_9$$

The problem was reduced to estimating the three parameters  $b_1$ ,  $b_2$  and  $b_3$  in each of the three systems.

The parameters thus obtained and their 95 per cent confidence intervals for the three systems are tabulated below. The program listings and the calculation of confidence intervals are included in Appendix D.

System	Parameter Values	95 per cent confidence intervals
Cumene	$b_1 = 2.2588 \times 10^2$	$1.9598 \times 10^2 \leq \beta_1 \leq 2.5578 \times 10^2$
	$b_2 = 1.3744 \times 10^{10}$	$1.1924 \times 10^{10} \leq \beta_2 \leq 1.5564 \times 10^{10}$
	$b_3 = 1.2048 \times 10^3$	$-1.0600 \times 10^{10} \leq \beta_3 \leq 1.0600 \times 10^{10}$
Cyclohexene	$b_1 = 2.1638 \times 10^2$	$1.7758 \times 10^2 \leq \beta_1 \leq 2.5518 \times 10^2$
	$b_2 = 1.3744 \times 10^{10}$	$1.1274 \times 10^{10} \leq \beta_2 \leq 2.6214 \times 10^{10}$
	$b_3 = 1.0500 \times 10^3$	$-1.1280 \times 10^{10} \leq \beta_3 \leq 1.1200 \times 10^{10}$
Tetralin	$b_1 = 1.9584 \times 10^2$	$-2.1042 \times 10^3 \leq \beta_1 \leq 2.5058 \times 10^3$
	$b_2 = 3.6280 \times 10^9$	$3.0140 \times 10^9 \leq \beta_2 \leq 4.2419 \times 10^9$
	$b_3 = 1.8140 \times 10^9$	$1.1326 \times 10^9 \leq \beta_3 \leq 2.4954 \times 10^9$

An examination of the confidence intervals indicates that the parameter values are all positive in the confidence region. This is one of the important criteria for model selection.

#### 4.2 Residual Analysis:

The residual analysis is a simple but powerful tool to test the adequacy of a model. A residual is the difference

between an observed value and the corresponding predicted value. Using the estimated parameters, rates were predicted (Appendix D3). The residuals were then obtained by subtracting the predicted rates from the observed ones. Figures 13, 14 and 15 show the residual plots against the independent variable viz. hydrocarbon concentration for the systems cumene, cyclohexene and tetralin, respectively. The plots show a random behaviour of the residuals which further substantiates the model.

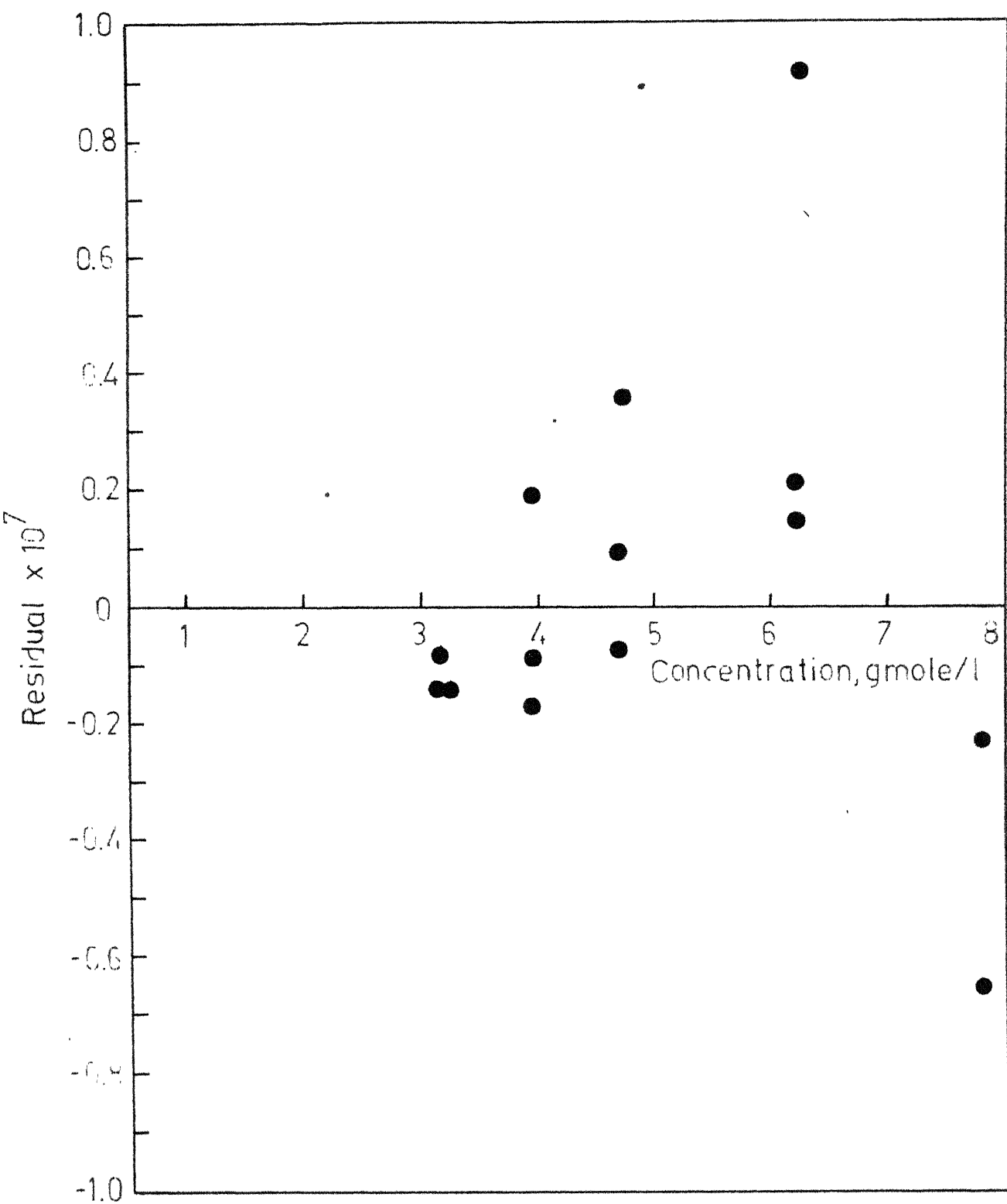


Fig. 13 -Plot of the residuals against the hydrocarbon concentration for the system cumene.



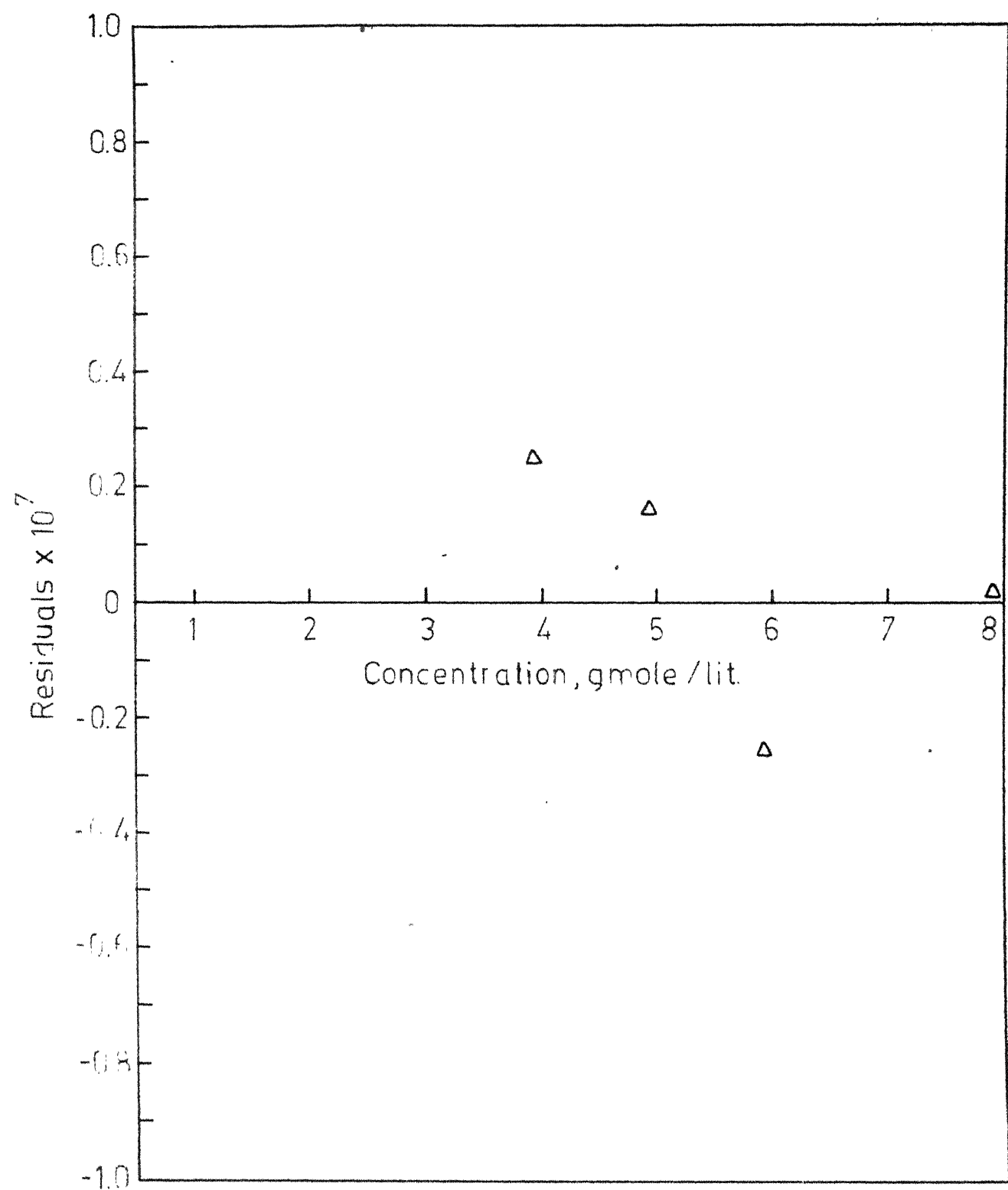


Fig. 14 - Plot of the residuals against hydrocarbon concentration for the system cyclohexene.

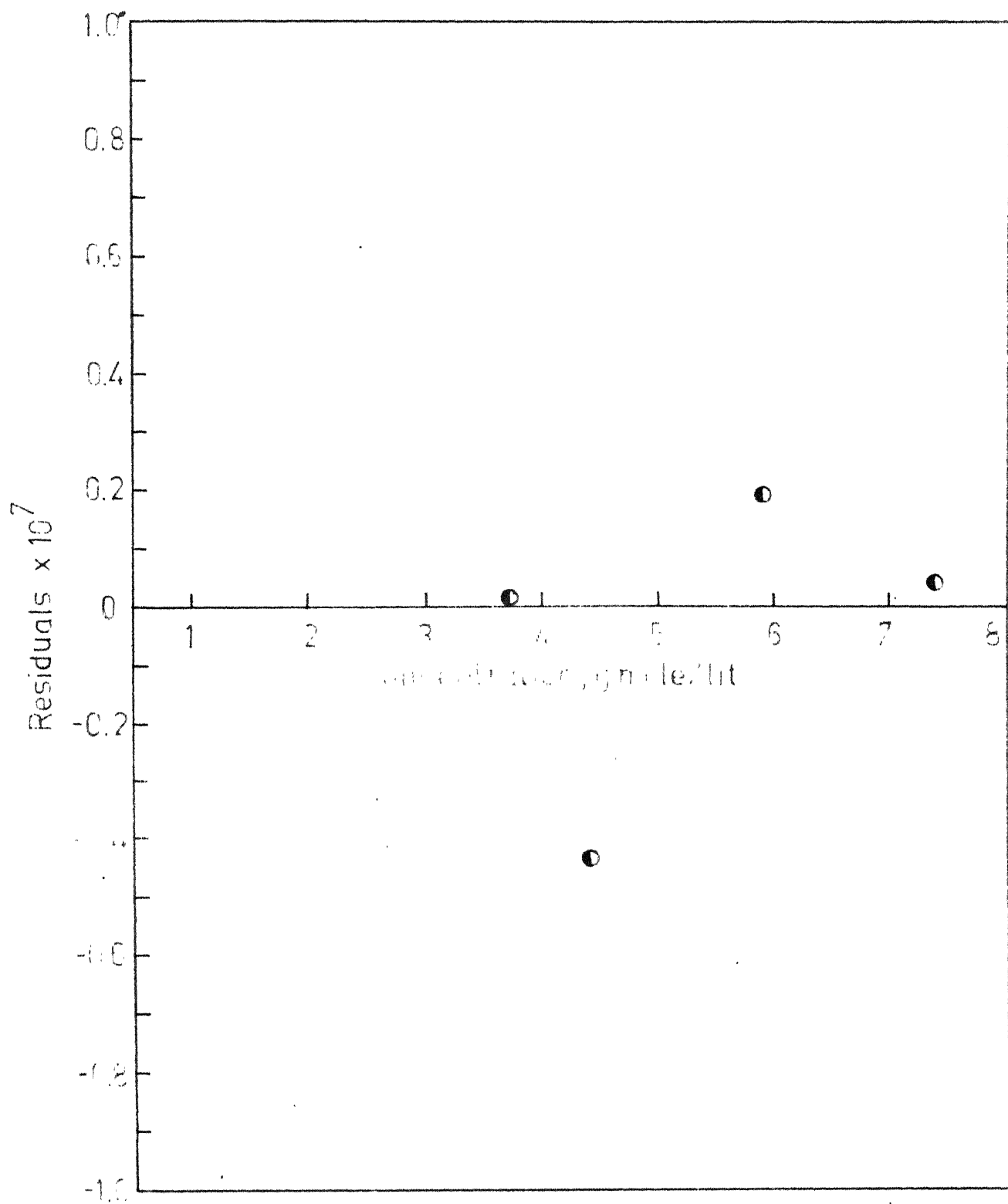


Fig 15 - Plot of residuals against the hydrocarbon concentration for the system tetralin.

## 5. CONCLUSIONS

The kinetics of oxidation of the three systems - cumene, cyclohexene and tetralin showed a similar behaviour. In all the three cases it was established that as the catalyst to hydrocarbon ratio was increased, the rate of oxygen absorption increased and after a certain ratio the rate declined suddenly. While an order of one with respect to hydrocarbon concentration was established earlier in the region before the break-in-point, a second order rate dependence on hydrocarbon concentration was obtained in the inhibiting region. The second order dependence in the inhibiting region supports the degenerate chain-branching mechanism.

The observed data were given a statistical treatment to test the adequacy of the model. The parameters were estimated using Rosenbrock's optimization method. The confidence intervals were also estimated. The parameters were all positive in the confidence region. Finally, a residual analysis showed a random nature with respect to the independent variable, hydrocarbon concentration. The positive nature of the parameters and the random behaviour of the residuals substantiate the model derived on the basis of degenerate chain-branching mechanism. Thus, such model, in general, accounts for the reactions where hydroperoxide forms and propagates the chain reaction.

---

## REFERENCES

1. Mukhorjee, A., and Graydon, W.F., J. Phys. Chem. 71, 4232 (1967).
2. Van Ham, N.H.A., Nieuwenhuys, B.E., and Sachtler, W.M.H., J. Catal., 20, 408-423 (1971).
3. Neuburg, H.J., Bassett, J.M., and Graydon, W.F., J. Catal. 25, 425-433 (1972).
4. Casemier, J.H.R., Nieuwenhuys, B.E., and Sachtler, W.M.H., J. Catal. 29, 367-373 (1973).
5. Varma, G.R., and Graydon, W.F., J. Catal. 28, 236-244 (1973).
6. Neuburg, H.J., Phillips, M.J., and Graydon, W.F., J. Catal. 33, 355-364 (1974).
7. Neuburg, H.J., Phillips, M.J., and Graydon, W.F., J. Catal. 38, 33-46 (1975).
8. Srivastava, R.K., and Srivastava, R.D., J. Catal. 39, 317-323 (1975).
9. Panayotova, E.N., Dimitrov, D.I., and Petkov, A.A., J. Catal. 41, 329-332 (1976).
10. Agarwal, A.K., and Srivastava, R.D., J. Catal. 45, 86-93 (1976).
11. Bolland, J.L., Proc. Roy. Soc. (London), A186, 220 (1946).
12. Wagner, C.D., Smith, R.H., and Peters, E.D., Anal. Chem. 19, 976 (1947).
13. Tokio Kato, Kogyo Kagaku Zasshi, 66, 31 (1963); Chem. Abs., 59, 57771b (1963).

14. Himmelblau, D.M. , Process Analysis by Statistical Methods, John Wiley and Sons, Inc., 1970.
  15. Draper, N.R., and Smith, H., Applied Regression Analysis, John Wiley and Sons, Inc., 1966.
  16. Beveridge, G., and Schechter, R.S., Optimization - Theory and Practice, McGraw Hill, New York, 1970.
  17. Mitchell, J. Jr., Kolthoff, I.M., Proskauer, E.S., and Weissberger, A., Organic Analysis, Vol. I, Interscience Publishers, Inc., New York, 1953.
-

APPENDIX A

CUMENE RUNS

TABLE A-1: OXYGEN ABSORPTION VERSUS TIME AT DIFFERENT  $\text{MnO}_2$   
CATALYST WEIGHTS AT  $80^\circ\text{C}$

Run No.	Catalyst ratio, g/ml	Time, min.	Oxygen consumption (g mole/ml) $\times 10^4$	Initial rate, g mole/sec $\times 10^7$
C-1	0.02	0	0	1.934
		5	0.602	
		10	1.160	
		15	1.722	
		20	2.250	
		25	2.940	
		30	3.364	
		35	3.785	
		40	4.080	
C-2	0.06	0	0.000	3.600
		5	1.080	
		10	2.065	
		15	2.940	
		20	3.505	
		25	3.880	
		30	4.020	
		35	4.235	
		40	4.315	

Table A-1 (contd)

Run No.	Catalyst ratio, g/ml	Time, min.	Oxygen consumption, (g mole/ml) x 10 <sup>4</sup>	Initial rate $\frac{\text{g mole}}{\text{sec}}$ x 10 <sup>7</sup>
C-3	0.10	0	0.000	4.170
		5	1.340	
		10	2.412	
		15	3.205	
		20	3.719	
		25	4.100	
		30	4.290	
		35	4.480	
C-4	0.14	0	0.000	5.170
		5	1.763	
		10	3.055	
		15	3.840	
		20	4.310	
		25	4.520	
		30	4.660	
C-5	0.160	0	0.000	4.800
		5	1.384	
		10	2.550	
		16.5	3.449	
		20	3.719	
		25	4.025	
		30	4.220	
		35	4.340	
		40	4.440	



Table A-1 (contd)

Run No.	Catalyst ratio, g/ml	Time, min.	Oxygen consumption, (g mole/ml) $\times 10^4$	Initial rate, $\frac{\text{g mole}}{\text{sec}} \times 10^7$
C-6	0.18	0	0.000	4.380
		5	1.276	
		10	2.389	
		15	3.110	
		20	3.460	
		25	3.745	
C-7	0.20	0	0.000	2.866
		5	0.814	
		10	1.850	
		15	2.429	
		20	2.879	
		25	3.140	

TABLE A-2: OXYGEN ABSORPTION VERSUS TIME FOR DIFFERENT CUMENE CONCENTRATIONS (LIMITING ZONE)

Run No.	Catalyst ratio, g/ml	Cumene concentration, g mole/lit	Time, min.	Oxygen absorption, $\frac{\text{g mole}}{\text{ml}} \times 10^4$	Initial rate, $\frac{\text{g mole}}{\text{sec}} \times 10^7$
C-8	0.16	7.82	0	0.000	4.800
			5	1.384	
			10	2.550	
			16.5	3.449	
			20	3.719	
			25	4.025	
			30	4.220	
			35	4.340	
			40	4.410	
C-9		6.26	0	0.000	4.130
			5	1.078	
			10.5	2.015	
			17	2.905	
			20	3.175	
			25	3.519	
			30	3.685	
			35	3.920	
C-10		4.69	0	0.000	1.731
			5	0.414	
			10	0.909	
			15	1.528	

Table A-2 (contd)

Run No.	Catalyst ratio, g/ml	Cumene concentration, g mole/lit	Time, min.	Oxygen absorption, $\frac{\text{g mole}}{\text{ml}} \times 10^4$	Initial rate, $\frac{\text{g mole}}{\text{sec}} \times 10^7$
C-11	3.99		20	1.928	1.142
			25	2.514	
			30	2.930	
			35	3.392	
			40	3.760	
			0	0.000	
			5	0.299	
			10	0.644	
			15	1.018	
			20	1.390	
			25	1.738	
C-12	0.16	3.13	30	2.049	0.667
			35	2.375	
			40	2.680	
			0	0.000	
			5	0.197	
			10	0.380	
			15	0.583	
			20	0.814	
			25	1.031	
			30	1.261	
			35	1.471	
			40	1.710	

Table A-2 (contd)

Run No.	Catalyst ratio, g/ml	Cumene concentration, g mole/bit	Time, min.	Oxygen absorption, $\frac{\text{g mole}}{\text{ml}} \times 10^4$	Initial rate, $\frac{\text{g mole}}{\text{sec}} \times 10^7$
C-13	0.18	7.82	0	0.000	4.380
			5	1.276	
			10	2.389	
			15	3.110	
			20	3.460	
			25	3.745	
C-14		6.26	0	0.000	3.430
			5	1.004	
			10	1.940	
			15	2.640	
			20	3.230	
			25	3.550	
			30	3.810	
			35	3.990	
C-15		4.69	0	0.000	2.166
			5	0.634	
			10	1.229	
			15	1.754	
			20	2.209	
			25	2.691	
			30	3.135	
			35	3.520	

CENTRAL LIBRARY

Acc. No. 50811

Table A-2 (contd)

Run No.	Catalyst ratio, g/ml	Cumene concentration, g mole/lit	Time, min.	Oxygen absorption, $\frac{\text{g mole}}{\text{ml}} \times 10^4$	Initial rate, $\frac{\text{g mole}}{\text{sec}} \times 10^7$
C-16	0.18	3.99	0	0.000	1.220
			5	0.345	
			10	0.732	
			15	1.173	
			20	1.532	
			25	1.864	
			30	2.154	
			35	2.470	
			40	2.749	
C-17		3.13	0	0.000	0.667
			5	0.207	
			10	0.394	
			15	0.593	
			20	0.828	
			25	1.008	
			30	1.256	
			35	1.470	
			40	1.711	
C-18	0.20	6.26	0	0.000	3.365
			5	0.966	
			10	2.070	
			15	2.925	
			20	3.570	

Table A-2 (contd)

Run No.	Catalyst ratio, g/ml	Cumene concentration, g mole/lit	Time, min.	Oxygen absorption, $\frac{\text{g mole}}{\text{ml}} \times 10^4$	Initial rate, $\frac{\text{g mole}}{\text{sec}} \times 10^7$
C-19	0.20	4.69	25	3.990	1.900
			30	4.265	
			35	4.400	
			40	4.500	
			0	0.000	
			5	0.566	
			10	1.160	
			20	2.235	
			25	2.745	
			30	3.130	
C-20		3.99	35	3.465	1.500
			40	3.625	
			0	0.000	
			5	0.469	
			10	0.897	
			15	1.241	
			20	1.531	
			25	1.884	
			30	2.090	
			35	2.499	
			40	2.840	

Table A-2 (contd)

Run No.	Catalyst ratio, g/ml	Cumene concentration, g mole/lit	Time, min.	Oxygen absorption, $\frac{\text{g mole}}{\text{ml}} \times 10^4$	Initial rate, $\frac{\text{g mole}}{\text{sec}} \times 10^7$
C-21		3.13	0	0.000	0.716
			5	0.176	.
			10	0.401	
			15	0.704	
			20	0.870	
			25	1.090	
			30	1.318	
			35	1.657	
			40	1.815	

TABLE A-3: CUMENE HYDROPEROXIDE DECOMPOSITION AT 80°C FOR  
DIFFERENT CATALYST (MnO<sub>2</sub>) RATIOS

Run No.	Catalyst ratio, g/ml	Initial Concentration, $\mu$ mole/ml			Final Concentration, $\mu$ mole/ml			Hydroperoxide decomposition
		$\text{HPR}^+$	$\text{KET}^{++}$	$\text{ALC}^\alpha$	HPR	KET	ALC	
C-22	0.02	68.1	90	73.4	25.1	70.0	77.8	63.1
C-23	0.06	68.1	90	73.4	22.1	90.0	73.5	67.5
C-24	0.10	68.1	90	73.4	18.0	90.0	79.6	72.4
C-25	0.12	68.1	90	73.4	12.3	190.0	78.9	82.0
C-26	0.14	68.1	90	73.4	16.0	150.0	80.2	76.5
C-27	0.16	68.1	90	73.4	12.3	130.0	79.3	82.0
C-28	0.18	68.1	90	73.4	22.3	100.0	78.4	67.3
C-29	0.20	68.1	90	73.4	22.3	100.0	78.4	67.3
$^+$ Hydroperoxide		$^{++}$ Ketone		$^\alpha$ Alcohol				



APPENDIX B

CYCLOHEXENE RUNS

TABLE B-1: OXYGEN CONSUMPTION VERSUS TIME FOR DIFFERENT  $\text{MnO}_2$  CATALYST WEIGHTS AT  $60^\circ\text{C}$

Run No.	Catalyst ratio, g/ml	Time, min.	Oxygen absorption, $\frac{\text{g mole}}{\text{ml}} \times 10^4$	Initial rate, $\frac{\text{g mole}}{\text{sec}} \times 10^7$
C-30	0.08	0	0.000	1.335
		5	0.103	
		10	0.937	
		15	1.756	
		20	2.270	
C-31	0.12	0	0.000	2.000
		5	0.571	
		8	0.780	
		10	0.908	
		15	1.274	
C-32	0.18	0	0.000	2.500
		5	0.586	
		10	0.835	
		15	1.180	
		20	1.370	
C-33	0.20	0	0.000	3.000
		5	0.880	
		10	1.610	
		15	1.990	
		20	2.230	

Table B-1 (contd)

Run No.	Catalyst ratio, g/ml	Time, min.	Oxygen absor- ption, $\frac{\text{g mole}}{\text{ml}} \times 10^4$	Initial rate, $\frac{\text{g mole}}{\text{sec}} \times 10^7$
C-34	0.32	0	0.000	2.400
		5	0.464	
		10	1.215	
		15	1.760	
		20	2.125	
C-35	0.40	0	0.000	1.500
		5	0.461	
		10	1.025	
		15	1.464	
		20	1.859	

TABLE B-2: OXYGEN CONSUMPTION VERSUS TIME FOR DIFFERENT CYCLO-  
HEXENE CONCENTRATIONS (LIMITING ZONE) AT 60°C

Run No.	Catalyst ratio, g/ml	Cyclohexene concentration, g mole/lit	Time, min.	Oxygen consumption $\frac{\text{g mole}}{\text{ml}} \times 10^4$	Initial rate $\frac{\text{g mole}}{\text{sec}} \times 10^7$
C-36	0.22	7.880	0	0.000	4.90
			5	1.377	
			10	2.254	
			15	2.750	
			20	3.149	
			25	3.380	
			30	3.540	
C-37	5.92	5.920	0	0.000	2.50
			5	0.615	
			10	1.464	
			15	2.250	
			20	2.855	
C-38		4.930	0	0.000	2.08
			5	0.659	
			10	1.518	
			15	1.918	
			20	2.430	
			25	2.955	
			30	3.395	

Table B-2 (contd)

Run No.	Catalyst ratio, g/ml	Cyclohexene concentration, g mole/lit	Time, min.	Oxygen con- sumption, $\frac{\text{g mole}}{\text{ml}} \times 10^4$	Initial rate $\frac{\text{g mole}}{\text{sec}} \times 10^7$
C-39		3.945	0	0.000	1.50
			5	0.439	
			10	0.922	
			15	1.428	
			20	1.889	
			25	2.320	
			30	2.755	

TABLE B-3: CHYCLOHEXENE HYDROPEROXIDE DECOMPOSITION AT 60°C FOR DIFFERENT CATALYST (MnO<sub>2</sub>) RATIOS

Run No.	Catalyst ratio, g/ml	Initial Concentration, $\mu$ mole/ml		Final Concentration		Per cent Hydroperoxide decomposition		
		HPR	KET	ALC	HPR		KLT	ALC
C-40	0.05	38	1490	$\underline{b}$	20	1180	$\underline{b}$	47.4
C-41	0.10	38	1490	$\underline{b}$	10	1020	$\underline{b}$	73.6
C-42	0.15	38	1490	$\underline{b}$	8	550	$\underline{b}$	79.0
C-43	0.25	38	1490	$\underline{b}$	22	1100	$\underline{b}$	42.0
C-44	0.30	38	1490	$\underline{b}$	16	900	$\underline{b}$	57.9
C-45	0.35	38	1490	$\underline{b}$	24	1360	$\underline{b}$	36.9

<sup>b</sup>Not estimated

APPENDIX C

TETRALIN RUNS

TABLE C-1: OXYGEN CONSUMPTION VERSUS TIME FOR DIFFERENT  $\text{MnO}_2$  CATALYST WEIGHTS AT  $65^\circ\text{C}$ 

Run No.	Catalyst ratio, g/ml	Time, min.	Oxygen consumption, $\frac{\text{g mole}}{\text{ml}} \times 10^4$	Initial rate $\frac{\text{g mole}}{\text{sec}} \times 10^7$
C-47	0.2	0	0.000	3.6
		5	1.081	
		10	1.750	
		15	2.300	
		20	2.800	
C-48	0.4	0	0.000	6.6
		5	2.065	
		10	3.500	
		15	4.500	
		20	5.100	
C-49	0.8	0	0.000	10.1
		5	1.514	
		10	2.600	
		15	3.300	
		20	4.000	
C-50	0.9	0	0.000	9.6
		5	2.830	
		10	4.110	
		15	5.190	
		20	5.980	
C-51	1.0	0	0.000	0.600
		5	0.180	
		10	0.450	
		16	1.081	
		20	1.587	



Table C-2 (contd)

Run No.	Catalyst ratio, g/ml.	Tetralin concentration, g mole/lit	Time, min.	Oxygen consumption, $\frac{\text{g mole}}{\text{ml}} \times 10^4$	Initial Rate $\frac{\text{g mole}}{\text{sec}} \times 10^4$
			15	2.129	
			20	2.705	
			25	3.210	
			30	3.675	
			35	4.110	
			40	4.470	
C-55		3.69	0	0.000	3.00
			5	0.829	
			10	1.298	
			15	1.730	
			20	2.125	
			25	2.625	
			30	2.885	
			35	3.245	
			40	3.605	

TABLE C-3: TETRALIN HYDROPEROXIDE DECOMPOSITION AT 65°C FOR DIFFERENT CATALYST (MnO<sub>2</sub>) RATIOS

Run No.	Catalyst ratio, g/ml	Initial Concentration		Final Concentration (30 min run)		Per cent Hydroperoxide decomposition	
		HPR	$\mu$ mole/ml KET	ALC	HPR	KET	ALC
C-56	0.02	44.2	a	b	34.5	a	b
C-57	0.06	44.2	a	b	12.7	a	b
C-58	0.40	44.2	a	b	18.1	a	b
C-59	0.80	44.2	a	b	12.0	a	b
C-60	0.90	44.2	a	b	17.6	a	b
C-61	1.00	44.2	a	b	24.1	a	b

<sup>a</sup>Detected in infrared spectra

<sup>b</sup>Not estimated

## APPENDIX D

### STATISTICAL ANALYSIS

```

      II=II+1
      DX(II)=(X(1)*RH(II)**2)/(2.*X(2)+X(3)*CAT(II))
      DD2CJ=1,NN
20    CONTINUE
      FUNXCN=0.0
      DD30 I=1,N
      FUNXCN=FUNXCN+(10.**7*DX(I)-DX1(I))**2
30    CONTINUE
      RETURN
      END

C
C * * * * * ROS00010
C * * * * * ROS00020
C * * * * * ROS00030
C EVALUATION OF MAXIMUM/MINIMUM OF A FUNCTION BY ROSENBROCK METHOD ROS00040
C V* COMPONENTS OF ORTHOGONAL VECTORS ROS00050
C SUBPROGRAM FUNXCN DEFINES FUNCTION F(X,Z) AS F(0,Z) ROS00060
C X* UNKNOWN VARIABLES ROS00070
C Z* KNOWN PARAMETERS ROS00080
C N* NUMBER OF UNKNOWN VARIABLES,X ROS00090
C NN* NUMBER OF KNOWN PARAMETERS,Z ROS00100
C NS* NUMBER OF STAGES AFTER WHICH CALCULATION SEQUENCE IS TERMINATED ROS00110
C MAXMIN = ZERO FOR MAXIMIZATION AND ONE FOR MINIMIZATION ROS00120
C LIMIT = ZERO FOR FINITE LIMIT AND ONE FOR NO FINITE LIMIT ROS00130
C ALPHA* A POSITIVE MULTIPLYING FACTOR FOR INCREASING A SUCCESSFUL STEP ROS00140
C BETA* A POSITIVE MULTIPLYING FACTOR FOR DECREASING UNSUCCESSFUL STEPS ROS00150
C E* INITIAL STEP SIZE AT THE BEGINNING OF EACH STAGE ROS00160
C * * * * * ROS00170
U FL* VALUE OF FINITE LIMIT ROS00180
1  FORMAT(5I5,4F10.6) ROS00190
   READ 2,(X(I),I=1,N),((V(I,J),J=1,N),I=1,N) ROS00200
2  FORMAT(8F10.6) ROS00210
   PRINT 3, N,NS,E,ALPHA,BETA ROS00220
3  FORMAT(1X,50H*****//1X ROS00230
1,1H*,48X,1H*/1X,31H*   NUMBER OF VARIABLES (N) *,I6,12X,1H*/1X,3 ROS00240
21H*   NUMBER OF STAGES (NS)   *,I6,12X,1H*/1X,31H*   INITIAL TR ROS00250
31AL STEP (E)   *,F10.6,8X,1H*/1X,12H*   ALPHA *,F10.6,3X,6HBETA * ROS00260
4,F10.6,8X,1H*/1X,1H*,48X,1H*/1X,50H*****//) ROS00270
5*****//) ROS00280
   IF(MAXMIN.EQ.0) GO TO 11 ROS00290
   IF(LIMIT.EQ.0) GO TO 13 ROS00300
   PRINT 10 ROS00310
   GO TO 17 ROS00320
4  CALL MINMAX(N,NS,MAXMIN,LIMIT,ALPHA,BETA,E,FL,X,V,Z) ROS00330
   GO TO 8 ROS00340
5  READ 6,(Z(I),I=1,NN) ROS00350
6  FORMAT(8F10.6) ROS00360
   PRINT 7,(Z(I),I=1,NN) ROS00370
7  FORMAT(//7X,3HZ *,8F15.8) ROS00380
   GO TO 4 ROS00390
8  PRINT 9 ROS00400

```

9	FORMAT(//47X,35HCOMPLETED REQUIRED NUMBER OF STAGES//)	RDS00410
	STOP	RDS00420
10	FORMAT(1H0,33HMINIMIZATION WITH NO FINITE LIMIT)	RDS00430
11	IF(LIMIT.EQ.0) GO TO 15	RDS00440
	PRINT 12	RDS00450
	GO TO 17	RDS00460
12	FORMAT(1H0,33HMAXIMIZATION WITH NO FINITE LIMIT)	RDS00470
13	PRINT 14, FL	RDS00480
	GO TO 17	RDS00490
14	FORMAT(1H0,35HMINIMIZATION WITH FINITE LIMIT FL =,F10.6)	RDS00500
15	PRINT 16, FL	RDS00510
16	FORMAT(1H0,35HMAXIMIZATION WITH FINITE LIMIT FL =,F10.6)	RDS00520
17	IF(NN.GT.0) GO TO 5	RDS00530
	GO TO 4	RDS00540
	END	RDS00550
C		RDS00560
	SUBROUTINE MINMAX(N,NS,MAXMIN,LIMIT,ALPHA,BETA,E,FL,X,V,Z)	RDS00570
	DIMENSION A(40,40),B(40,40),C(40,40),P(40,40),V(40,40)	RDS00580
	DIMENSION D(40),O(40),R(40),X(40),Y(40),Z(40)	RDS00590
	S=E	RDS00600
	L=1	RDS00610
	NSTAGE=-1	RDS00620
	NTRIAL=-1	RDS00630
	NSUXES=0	RDS00640
	NFELUR=0	RDS00650
	DO 1 I=1,N	RDS00660
	D(I)=0.0	RDS00670
	O(I)=X(I)	RDS00680
	R(I)=0.0	RDS00690
	Y(I)=0.0	RDS00700
	DO 1 J=1,N	RDS00710
	A(I,J)=0.0	RDS00720
	B(I,J)=0.0	RDS00730
	C(I,J)=0.0	RDS00740
1	P(I,J)=0.0	RDS00750
2	F=FUNXON(O,Z,N)	RDS00760
	IF(NTRIAL.LT.0) GO TO 9	RDS00770
	IF(MAXMIN.EQ.0) GO TO 15	RDS00780
	IF(LIMIT.EQ.0) GO TO 18	RDS00790
3	IF(F.LE.FM) GO TO 13	RDS00800
4	IF(NSTAGE.LT.0) GO TO 5	RDS00810
	NFELUR=NFELUR+1	RDS00820
	IF(NSUXES.GT.0) GO TO 21	RDS00830
5	E=-BETA*E	RDS00840
6	NTRIAL=NTRIAL+1	RDS00850
	Y(L)=E	RDS00860
	DO 8 I=1,N	RDS00870
	O(I)=0.0	RDS00880
	DO 7 J=1,N	RDS00890
7	O(I)=O(I)+V(I,J)*Y(J)	RDS00900

8	O(I)=O(I)+X(I)	ROS00910
	GO TO 2	ROS00920
9	NTRIAL=NTRIAL+1	ROS00930
	PRINT 10,F,(X(I),I=1,N)	ROS00940
10	FORMAT(/1X,21H **STARTING VALUES**//7X,3HF *,F15.8//7X,3HX *,	ROS00950
	1RF15.8)	ROS00960
	PRINT 11	ROS00970
11	FORMAT(/7X,3HV *)	ROS00980
	PRINT 12,((V(I,J),J=1,N),I=1,N)	ROS00990
12	FORMAT(10X,4F15.8/)	ROS01000
13	FM=F	ROS01010
	IF(NSTAGE.LT.0) GO TO 19	ROS01020
	D(L)=D(L)+Y(L)	ROS01030
	DO 14 I=1,N	ROS01040
14	X(I)=O(I)	ROS01050
	NSUXES=NSUXES+1	ROS01060
	IF(NFELUR.GT.0) GO TO 21	ROS01070
	E=ALPHA*E	ROS01080
	GO TO 6	ROS01090
15	IF(LIMIT.EQ.0) GO TO 16	ROS01100
	GO TO 17	ROS01110
16	IF(F.LE.FL) GO TO 17	ROS01120
	GO TO 4	ROS01130
17	IF(F.GE.FM) GO TO 13	ROS01140
	GO TO 4	ROS01150
18	IF(F.GE.FL) GO TO 3	ROS01160
	GO TO 4	ROS01170
19	NSTAGE=NSTAGE+1	ROS01180
	GO TO 6	ROS01190
21	Y(L)=0.0	ROS01200
	L=L+1	ROS01210
	IF(L.GT.N) GO TO 23	ROS01220
22	F=S	ROS01230
	NSUXES=0	ROS01240
	NFELUR=0	ROS01250
	GO TO 6	ROS01260
23	NSTAGE=NSTAGE+1	ROS01270
	CALL VECTOR(A,B,C,P,V,D,R,N)	ROS01280
	TEMP1=R(1)	ROS01290
	TEMP2=0.0	ROS01300
	DO 24 I=1,N	ROS01310
24	TEMP2=TEMP2+A(I,2)**2	ROS01320
	TEMP2=SQRT(TEMP2)/TEMP1	ROS01330
	PRINT 25, NSTAGE, NTRIAL, F, TEMP1, TEMP2, (X(I), I=1, N)	ROS01340
25	FORMAT(/21H AT THE END OF STAGE ,I6,9H AND ,I6,9H TRIALS//7R	ROS01350
	1X,3HF *,F15.8//2X,8HMAG A1 *,F15.8,5X,14HMAG A2/MAG A1*,F15.8//7X,	ROS01360
	23HX *,8F15.8)	ROS01370
	PRINT 26	ROS01380
26	FORMAT(/7X,3HV *)	ROS01390
	PRINT 27,((V(I,J),J=1,N),I=1,N)	ROS01400

27	FORMAT(10X,4F15.8/)	ROS01411
	IF(NSTAGE.EQ.NS) GO TO 29	ROS01421
	DO 28 I=1,N	ROS01431
	D(I)=0.0	ROS01441
	R(I)=0.0	ROS01451
	Y(I)=0.0	ROS01461
	DO 28 J=1,N	ROS01471
	A(I,J)=0.0	ROS01481
	B(I,J)=0.0	ROS01491
	C(I,J)=0.0	ROS01501
28	P(I,J)=0.0	ROS01511
	L=1	ROS01521
	GO TO 22	ROS01531
29	RETURN	ROS01541
	END	ROS01551
C		ROS01561
	SUBROUTINE VECTOR(A,B,C,P,V,D,R,N)	ROS01571
	DIMENSION A(40,40),B(40,40),C(40,40),P(40,40),V(40,40)	ROS01581
	DIMENSION D(40),R(40)	ROS01591
	DO 1 J=1,N	ROS01601
	DO 1 I=1,N	ROS01611
	DO 1 K=J,N	ROS01621
1	A(I,J)=A(I,J)+D(K)*V(I,K)	ROS01631
	DO 2 I=1,N	ROS01641
	B(I,1)=A(I,1)	ROS01651
2	R(1)=R(1)+B(I,1)**2	ROS01661
	R(1)=SQRT(R(1))	ROS01671
	DO 3 I=1,N	ROS01681
3	V(I,1)=B(I,1)/R(1)	ROS01691
	DO 8 J=2,N	ROS01701
	MJ=J-1	ROS01711
	DO 4 K=1,MJ	ROS01721
	DO 4 I=1,N	ROS01731
4	C(J,K)=C(J,K)+A(I,J)*V(I,K)	ROS01741
	DO 6 L=1,MJ	ROS01751
	DO 6 I=1,N	ROS01761
	P(I,J)=P(I,J)+C(J,1)*V(I,L)	ROS01771
6	B(I,J)=A(I,J)-P(I,J)	ROS01781
	DO 7 I=1,N	ROS01791
7	R(J)=R(J)+B(I,J)**2	ROS01801
	R(J)=SQRT(R(J))	ROS01811
	DO 8 I=1,N	ROS01821
8	V(I,J)=B(I,J)/R(J)	ROS01831
	RETURN	ROS01841
	END	ROS01851
C		ROS01861
	FUNCTION FUNXON(O,Z,N)	ROS01871
C	VARIABLE X(I) IS TEMPORARILY SUBSTITUTED BY VARIABLE O(I)	ROS01881
	DIMENSION O(40),Z(40)	ROS01891
	FUNXON=100.*(O(2)-O(1)*O(1))**2+(1.-O(1))**2	ROS01901

RETURN  
FIELD

C

ROS01910  
ROS01920  
ROS01930  
ROS01940  
ROS01950



APPENDIX D2CONFIDENCE INTERVAL CALCULATION FOR PARAMETER ESTIMATES

The confidence intervals for the parameters were calculated from the observations as follows:

1. The first order partial derivatives of the rate expression with respect to each of the parameters were obtained.
2. The numerical values of the derivatives were obtained by substituting the values of independent variables i.e. concentration and catalyst ratio and the estimated values of parameters. The values were written in the form of a  $n \times m$  matrix. This  $n \times m$  matrix is denoted by  $x$  where  $m$  being number of parameters and  $n$  being number of observations.

Let

$$R = \frac{b_1 [RH]^2}{b_2 + b_3 [M]}$$

be the rate expression.

Differentiating with respect to  $b_1$ ,

$$\left(\frac{\partial R}{\partial b_1}\right) = \frac{[RH]^2}{b_2 + b_3 [M]}$$

Similarly, the other two derivatives are

$$\left(\frac{\partial R}{\partial b_2}\right) = \frac{-b_1 [RH]^2}{(b_2 + b_3 [M])^2}$$

$$\left(\frac{\partial R}{\partial b_3}\right) = \frac{-b_1 [RH]^2 [M]}{(b_2 + b_3 [M])^2}$$

The matrix is of the form

$$X = \begin{bmatrix} \left(\frac{\partial R}{\partial b_1}\right)_1 & \left(\frac{\partial R}{\partial b_2}\right)_1 & \left(\frac{\partial R}{\partial b_3}\right)_1 \\ \text{---} & \text{---} & \text{---} \\ \text{---} & \text{---} & \text{---} \\ \left(\frac{\partial R}{\partial b_1}\right)_n & \left(\frac{\partial R}{\partial b_2}\right)_n & \left(\frac{\partial R}{\partial b_3}\right)_n \end{bmatrix}$$

Where the subscript indicates the number of experimental observation. For example, in case of cumene a 14 x 3 matrix was obtained as 14 was the number of experimental observations.

3.  $[X^T X]^{-1}$  was obtained by inverting  $[X^T X]$ .  $[X^T X]^{-1}$  was a 3 x 3 matrix in all the cases.

$$c = [X^T X]^{-1} = \begin{bmatrix} c_{11} & c_{12} & c_{13} \\ c_{21} & c_{22} & c_{23} \\ c_{31} & c_{32} & c_{33} \end{bmatrix}$$

A typical  $[X^T X]^{-1}$  for the system cumene was,

$$\begin{bmatrix} 0.12508 \times 10^{18} & 0.76112 \times 10^{25} & 0.4426 \times 10^{26} \\ 0.76112 \times 10^{25} & 0.46311 \times 10^{33} & -0.26933 \times 10^{34} \\ 0.44264 \times 10^{26} & -0.26933 \times 10^{34} & 0.37569 \times 10^{35} \end{bmatrix}$$

The parameter values for cumene obtained by Rosenbrock optimization procedure are as

$$b = \begin{bmatrix} 2.2588 \times 10^2 \\ 1.3744 \times 10^{10} \\ 1.2048 \times 10^3 \end{bmatrix}$$

The individual parameter confidence intervals were calculated using the equations

$$b_1 - t_{1-\frac{\alpha}{2}} s_{\bar{y}_i} \sqrt{c_{11}} \leq \beta_1 < b_1 + t_{1-\frac{\alpha}{2}} s_{\bar{y}_i} \sqrt{c_{11}}$$

$$b_2 - t_{1-\frac{\alpha}{2}} s_{\bar{y}_i} \sqrt{c_{22}} \leq \beta_2 < b_2 + t_{1-\frac{\alpha}{2}} s_{\bar{y}_i} \sqrt{c_{22}}$$

$$b_3 - t_{1-\frac{\alpha}{2}} s_{\bar{y}_i} \sqrt{c_{33}} \leq \beta_3 < b_3 + t_{1-\frac{\alpha}{2}} s_{\bar{y}_i} \sqrt{c_{33}}$$

where

$s_{\bar{y}_i}$  - estimated variance of  $y$

$t_{1-\frac{\alpha}{2}}$  - value from 't' distribution corresponding to  
to a significant level of  $\alpha$  in a two sided  
test.

$s_{\bar{y}_i}$  was obtained from the expression

$$s_r = \sqrt{s_r^2} = \sqrt{\frac{RSS}{\gamma}}$$

where RSS - residual sum of squares

$\gamma$  - degrees of freedom

= (number of observations - number of parameters).

APPENDIX D3RESIDUAL ANALYSIS

TABLE D.1: SYSTEM-CUMENE

Observed Rate g mole/sec x 10 <sup>7</sup>	Predicted Rate g mole/sec x 10 <sup>7</sup>	Hydrocarbon concentration g mole/lit	Residual x 10 <sup>7</sup>
4.800	5.030	7.820	-0.230
4.130	3.220	6.260	0.910
1.730	1.810	4.690	-0.080
1.140	1.310	3.990	-0.170
0.667	0.805	3.130	-0.138
4.380	5.030	7.820	-0.650
3.430	3.220	6.260	0.210
2.170	1.810	4.690	0.360
1.220	1.310	3.990	-0.090
0.667	0.805	3.130	-0.138
3.370	3.220	6.260	0.150
1.900	1.810	4.690	0.090
1.500	1.310	3.990	0.190
0.718	0.805	3.130	-0.089

TABLE D-2: SYSTEM-CYCLOHEXENE

Observed Rate g mole/sec $\times 10^7$	Predicted Rate, g mole/sec $\times 10^7$	Hydrocarbon concentration g mole/lit	Residual $\times 10^7$
4.90	4.89	7.88	0.0119
2.50	2.76	5.92	-0.2590
2.08	1.91	4.93	0.1670
1.50	1.23	3.94	0.2570

TABLE D-3: SYSTEM-TETRALIN

Observed Rate, g mole/sec $\times 10^7$	Predicted Rate, g mole/sec $\times 10^7$	Hydrocarbon concentration g mole/lit	Residual $\times 10^7$
12.00	12.00	7.37	0.0350
7.84	7.64	5.89	0.1960
3.86	4.30	4.42	-0.4440
3.00	2.99	3.68	0.0081